

# 2

## The Respiratory System

---

Induced lesions of the respiratory tract are described on an organ-by-organ basis with illustrations. Both nonneoplastic and neoplastic changes of the various regions are covered. Examples of test articles causing different lesions are provided. Lesions of the upper respiratory tract in inhalation safety studies are described in some detail, with particular reference to their significance. The mechanisms of toxicity in the various regions of the tract are discussed briefly, along with their relationship to the pathogenesis of these changes. The relevance of certain mechanical and physiological features to the development of these lesions also is mentioned.

### 2.1 Introduction

---

The respiratory tract was recognised several decades ago as a major target for toxicity due to airborne pollutants. The increasing numbers of people affected by neoplastic and nonneoplastic pathologic conditions of the respiratory tract have made it a major area for research and for the targeting of therapeutic agents.

Inhalation toxicology initially gained importance as a technique to study the effects of environmental airborne pollutants on the respiratory tract, primarily for pulmonary changes. Compounds tested included cigarette smoke, toxic gases such as sulphur dioxide, occupationally inhaled chemicals and particles, solvents, dyes, and particles such as carbon, silica, and asbestos. The increasingly wide range of household products sold as aerosols, such as polishes, cleaning agents, hairsprays, and deodorants, also required safety evaluation to assess potential for damage to the respiratory tract.

More recently, a wide range of therapies including biologics has been developed for treating respiratory conditions via the inhalation route, notably antiasthmatics, treatments for chronic obstructive pulmonary disease and cystic fibrosis, and anti-allergics.

The structure and metabolic function of different areas of the respiratory tract have a bearing on the distribution and severity of induced toxicologic lesions [1, 2]. Several mechanical factors also cause or influence toxicity in studies of this type [3–5]. The size and shape of particles, particle density, and molecular weight are just a few of the factors that can determine the regions of the respiratory tract that may be affected and the nature and extent of their toxicity [6]. Recognition of these variables has initiated considerable interest in the morphology and physiology of the nasal passages. Inhalation toxicology in safety assessment is now an intensively studied field, with an extensive bibliography describing the range of neoplastic and nonneoplastic changes induced in animal models by different classes of pharmaceuticals and chemicals. In addition, transport of toxicants into the brain via the olfactory nerves is recognised and has aroused considerable interest [7].

Systemic administration of chemicals and pharmaceuticals, such as paraquat, bleomycin, and cyclophosphamide, also may produce changes in the respiratory system. Metabolism of xenobiotics may occur throughout the respiratory tract, such as in the nose, conducting passages, and airways, producing toxic metabolites. Specific types and concentrations of enzymes differ among regions, the site-specific localisation of enzymes accounting, at least partially, for regional susceptibility or resistance to injury. Enzymes in the respiratory tract include cytochromes P450 (CYPs), monooxygenases, dehydrogenases, prostaglandin

G synthetase, and phase II enzymes such as glucuronyl and glutathione transferases that facilitate excretion. Enzyme activity and metabolism are greatest in the olfactory mucosa and Clara cells of the bronchioles because of their high CYP content. Types I and II pneumocytes and endothelial cells have lower levels of activity.

Many agents produce toxicity in the respiratory tract by indirect mechanisms; for example, immunosuppressants may result in pneumonia. Impaired clearance mechanisms, such as impaired macrophage function

due to phospholipidosis, predispose to bacterial and fungal infections of the airways and lungs. Immune-mediated pathology due to type I or III hypersensitivity reactions also may occur.

To ensure consistent coverage of all susceptible areas of the respiratory tract in an inhalation study, a standard protocol should be followed for selecting, trimming, and examining respiratory organs. A terminology guide for pathologic changes in the respiratory tract in rodents also has been published recently [8].

## 2.2 Nasal Turbinates

To assess the turbinates thoroughly, three to four levels of the nasal passages should be examined, with the sectioning protocol designed to include squamous, transitional, respiratory, and olfactory epithelia. Sections should also include the different areas of turbinates and the vomeronasal organ [9, 10]. Distribution of lesions in the turbinates depends on various factors, including dose to the affected area, site-specific susceptibility, local metabolism, species, and sex [7, 11–13]. Areas affected may also depend on the physical and chemical nature of the test article [14].

Induced changes seen in the nasal turbinates are as follows:

- Eosinophilic inclusions (globules)
- Inflammation
- Disorganisation/degeneration/atrophy
- Erosion/ulceration
- Regeneration/hyperplasia
- Metaplasia, respiratory or squamous
- Vomeronasal organ—degeneration/necrosis
- Tumours—papillomas/adenomas/adenocarcinomas/squamous cell carcinomas/olfactory epithelial carcinoma
- Neuroendocrine cell tumours

Inhaled substances frequently cause histopathological changes localised to the nasal turbinates, as these are the first point of contact and receive a high concentration of the article. Changes may be caused by direct irritation due to their chemical nature or physical properties, or through toxicity by the test article or one of its metabolites. Arguably the commonest cause of lesions is direct irritation, which is caused by a wide range of chemicals, including formaldehyde and alachlor, and pharmaceuticals including  $\beta$ -agonists, Toll-like receptor agonists, and muscarinic antagonists.

The most rostral regions of the nasal cavity are lined by squamous epithelium, which is relatively resistant. Irritant compounds may induce inflammation, hyperplasia, and keratinisation, with erosion and ulceration seen with more strongly irritant materials (Fig. 2.1). The areas of rodent nasal mucosa that develop lesions most frequently are the transitional, respiratory, and olfactory epithelia lining the caudal third of the nasal and maxillary turbinates [8]. Low-grade irritation often results in minimal changes, such as epithelial eosinophilic inclusions in the respiratory and olfactory epithelium and goblet cell hyperplasia (Figs. 2.2 and 2.3) of the respiratory epithelium. Eosinophilic inclusions also may appear in the

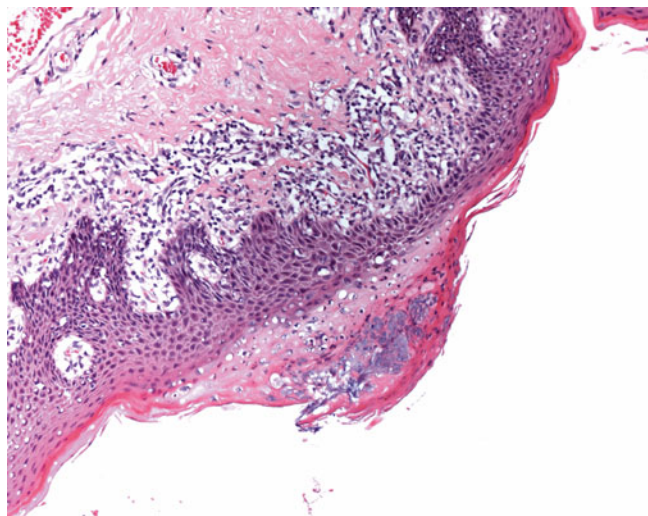


**FIGURE 2-1.** Focal epithelial erosion of the nasal turbinates in a monkey given an irritant pharmaceutical. Thinning of the squamous epithelium with submucosal lymphocytic infiltration and parakeratosis with nuclear debris and eosinophilic material are seen. Haematoxylin and eosin (H&E).

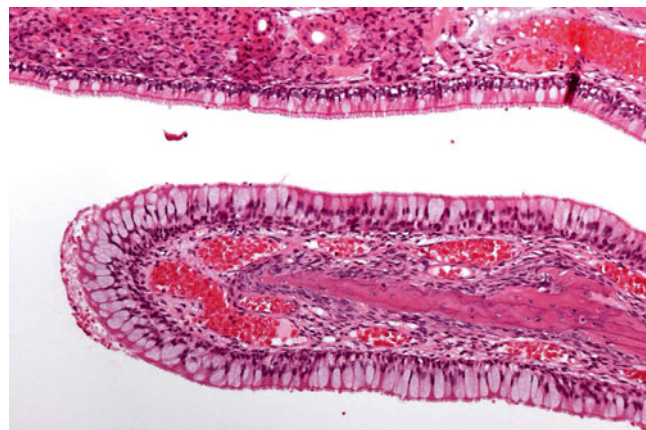


**FIGURE 2-2.** Goblet cell hyperplasia of the nasal turbinates from a rat given a  $\beta$ -adrenergic agent. The respiratory epithelium lining the turbinates is composed mainly of hypertrophic goblet cells. H&E.

epithelium of the submucosal glands and their ducts (Fig. 2.4). They may be located in any area of the cell, often becoming very large and displacing the nuclei. Ultrastructurally, they appear as membrane-bound ellipsoid bodies containing a homogenous electron-dense matrix. These droplets are negative for polysaccharides on staining by the periodic acid-Schiff (PAS) technique, Alcian blue, and several other stains [15]. They have been induced in rats by a wide range of chemicals and consist of xenobiotic-metabolising enzymes [16].

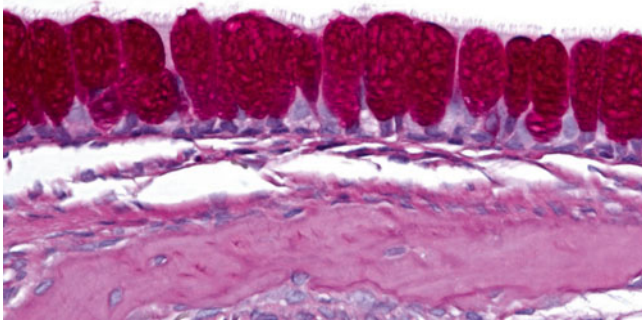


**FIGURE 2-3.** Goblet cell hyperplasia of the nasal turbinates from a rat given a  $\beta$ -adrenergic agent. The hypertrophic mucus-producing cells of the nasopharynx stain strongly positive for neutral mucopolysaccharides. PAS-Haematoxylin staining.

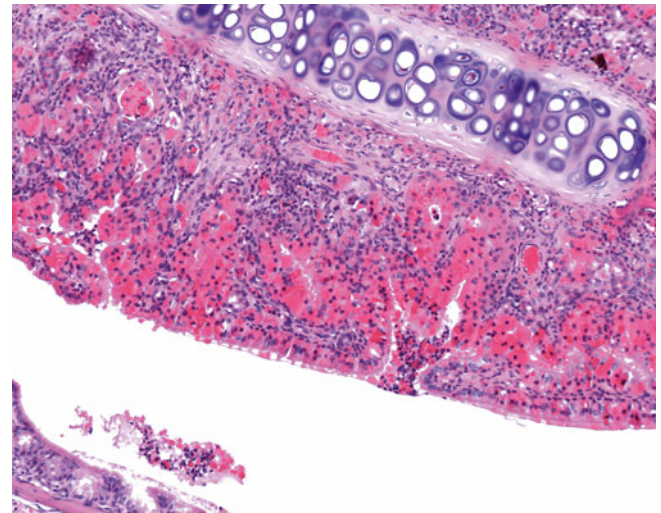


**FIGURE 2-4.** Eosinophilic droplets in the nasal turbinates of a mouse treated with a  $\beta$ -adrenergic agent. The respiratory epithelial cells contain eosinophilic droplets. Also present is marked diffuse hypertrophy of the septal submucosal glands due to distension of acinar and ductal cells with eosinophilic droplets, with mild interstitial inflammation and inflammatory debris in the glands and airways. H&E.

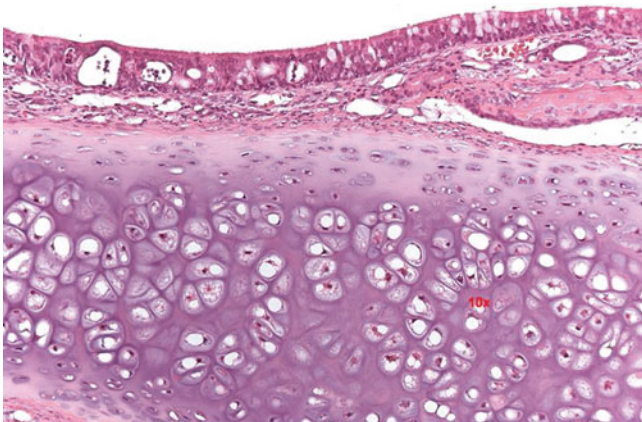


**FIGURE 2-5.** Mild inflammation in the nasal turbinates of a rat given an industrial chemical. Microabscess formation, disorganisation, minimal cell loss, and loss of cilia are present in the septal respiratory epithelium, which is minimally thickened. H&E.

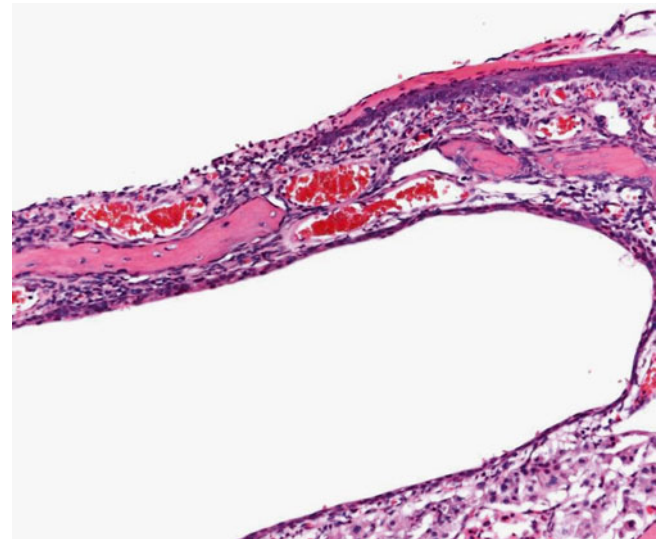


**FIGURE 2-6.** Ulceration and inflammation of the nasal turbinates from a rat given a muscarinic antagonist. The respiratory epithelium shows degeneration, inflammation, ulceration, and localised squamous metaplasia with keratinisation. This combination of changes is seen often with irritant compounds. H&E.



area (Fig. 2.7). The reparative epithelium matures into the original epithelial type or may develop into a more resistant epithelial type, such as respiratory to squamous. True squamous metaplasia, comprising multilayered squamous epithelium with superficial 'umbrella' cells, should be differentiated from the thin layer of flattened epithelial cells seen during early regeneration. Submucosal glands can also undergo inflammation, atrophy, and/or squamous metaplasia as a result of ductal inflammation or blockage (Fig. 2.8).

Ulceration with necrosis of the underlying soft tissues, and sometimes the turbinate bones, also may be induced. Repair results in the development of

adhesions, often with fusion of turbinates and subsequent distortion. Marked fibrosis with cartilaginous metaplasia progressing downwards from the dorsal meatus along the septum and extending laterally, involving the turbinates, and partially obliterating the lumen of the nasal cavity has been seen with an industrial chemical (Figs. 2.9 and 2.10).

The vomeronasal organ, or organ of Jacobson, is located at the base of the nasal septum, and is lined laterally by olfactory epithelium and medially by respiratory columnar epithelium. It has important sensory functions in animals. Irritant compounds, such as muscarinics, produce degeneration and necrosis of both epithelial

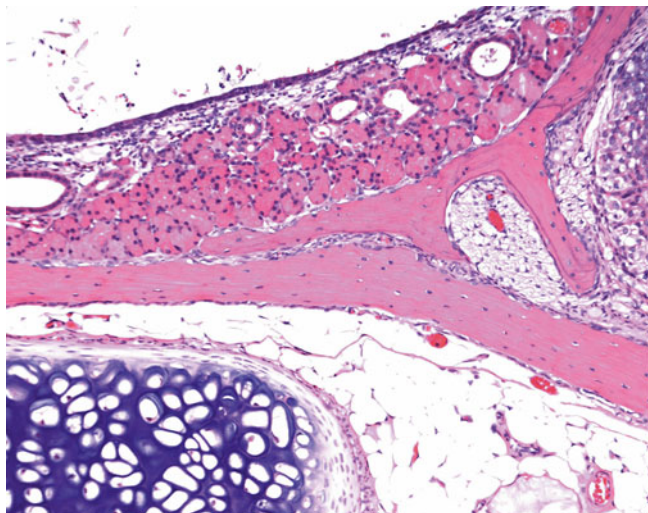


**FIGURE 2-7.** Regenerating epithelium in the nasal turbinates of a rat given a muscarinic antagonist. A layer of regenerating cuboidal basophilic epithelial cells lines the nasal septum, representing regeneration of the normal respiratory epithelium. Inflammatory cells are present in the lamina propria. H&E.

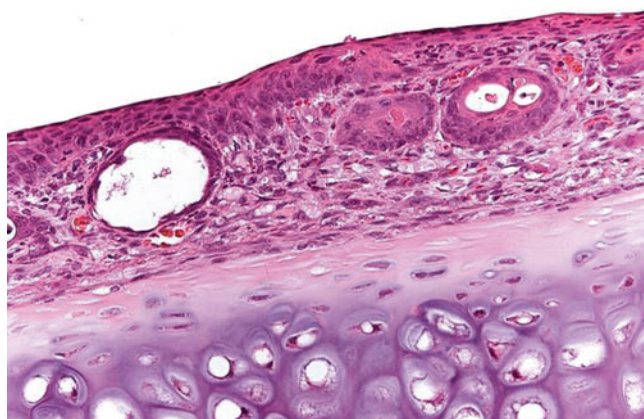


**FIGURE 2-8.** Squamous metaplasia in the nasal turbinates of a rat given a muscarinic antagonist. Mature squamous epithelium has completely replaced the normal respiratory epithelium of the septum. The submucosal glands and ducts also have undergone squamous metaplasia. H&E.

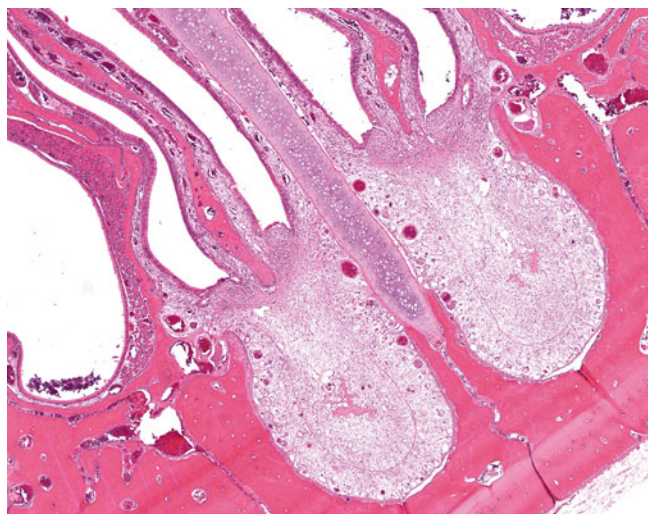


**FIGURE 2-9.** Severe fibrosis in the nasal cavity of a rat given an inhaled industrial chemical. The normal structures and lumen of the dorsal meatus have been completely replaced by fibrous proliferation. The respiratory epithelium has healed over the fibrotic areas. H&E.

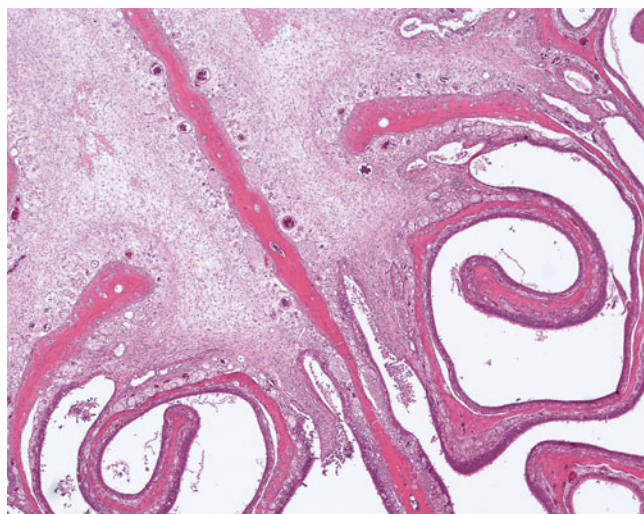


**FIGURE 2-10.** Fibrosis with early cartilaginous metaplasia in the nasal turbinates of a rat given an inhaled industrial chemical. Fibrosis has partially occluded the nasal cavity, involving the ethmoturbinates. Early cartilaginous differentiation is present in the fibrotic tissue. H&E.



types (Fig. 2.11), with subsequent regeneration of either the original epithelium or squamous metaplasia.

In our experience, changes in the olfactory epithelium due to irritation are most frequently localised to the rostral portion of the dorsal medial meatus of the turbinates, sometimes extending laterally along the dorsal ethmoid turbinates and less frequently along the medial septum. This distribution is similar to that noted by other authors [7, 17]. The ethmoid turbinates often are largely unaffected.

Low-grade irritation may induce eosinophilic droplets in the olfactory epithelium of rodents; however, these are also seen as a spontaneous finding, especially in

older animals (Fig. 2.12). More marked induced changes seen in the olfactory epithelium include inflammation, disorganisation, atrophy, apoptosis, degeneration, and necrosis (Fig. 2.13). Olfactory epithelial atrophy, notably in rodents, is frequently associated with atrophy of the underlying nerve bundles and, sometimes, atrophy of the Bowman's glands lying between these bundles (Fig. 2.14). Because of its capacity for regeneration by replication of the basal cell layer, regenerative olfactory epithelial hyperplasia may accompany ongoing degenerative processes. If the insult is prolonged, respiratory or squamous epithelium may replace the olfactory epithelium (Fig. 2.15).

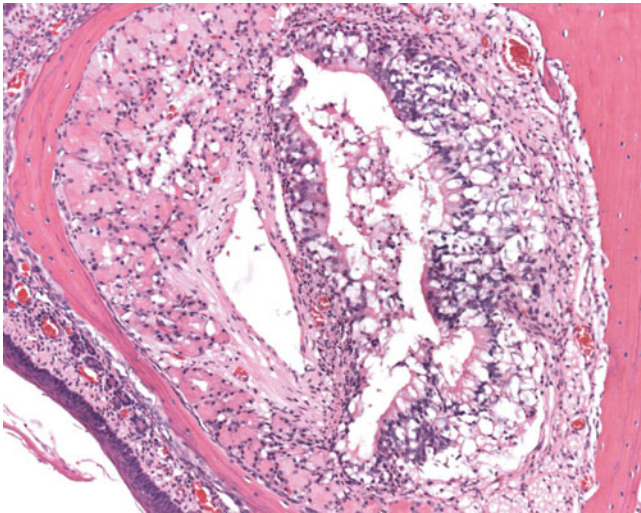


**FIGURE 2-11.** Necrosis of the vomeronasal organ from a rat given a muscarinic antagonist. Marked degeneration, necrosis, and desquamation of the olfactory and columnar epithelium are present. Inflammatory cells are scattered in the lamina propria, and cellular debris is seen in the lumen. H&E.

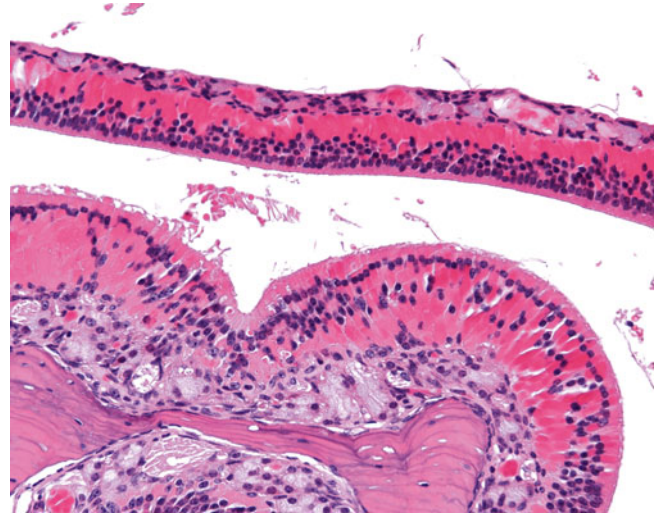


**FIGURE 2-12.** Eosinophilic droplets in the nasal turbinates of a rat given a  $\beta$ -adrenergic agonist in a long-term study. The olfactory epithelium of the ethmoturbinates is moderately hypertrophic, with loss of architecture. Large eosinophilic droplets have displaced the epithelial nuclei dorsally. H&E.

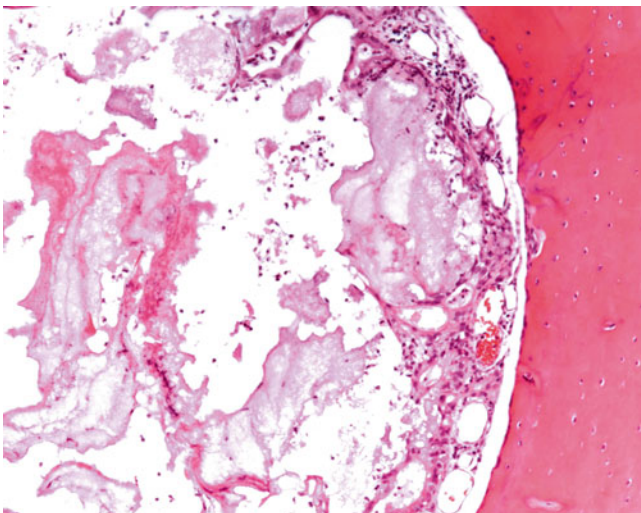


**FIGURE 2-13.** Degeneration and ulceration of the nasal turbinates in a rat given a biologic. Marked degeneration, erosion, ulceration, and inflammation of the olfactory epithelium are seen at the dorsal meatus, with marked eosinophilic material and cellular debris in the lumen. H&E.

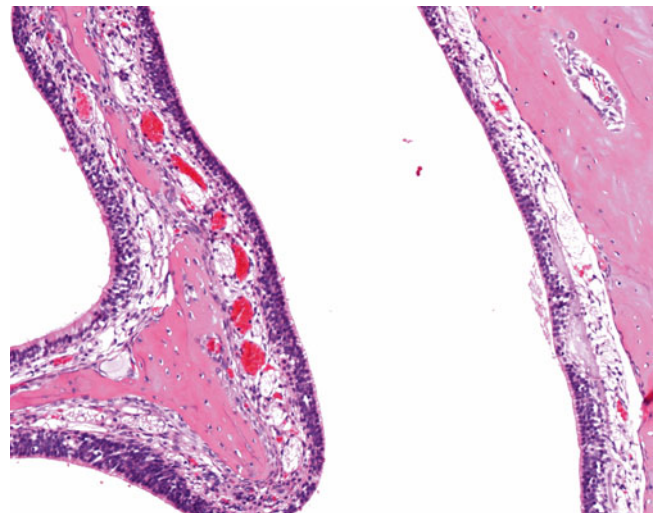


**FIGURE 2-14.** Atrophy of the nasal turbinates in a rat that received an inhaled industrial chemical. The olfactory epithelium at the dorsal meatus shows moderate atrophy, with almost complete loss of the underlying nerve bundles and Bowman glands. Corpora amylacea are present along the basement membrane. H&E.

In addition, metabolism of inhaled xenobiotics by the olfactory epithelium, because of its high content of mixed function CYP oxidases—and occasionally, metabolism by associated structures, such as Bowman's glands—can generate toxic metabolites. This results in diffuse atrophy, degeneration, and atrophy of the olfactory epithelium, which is most evident on the ethmoid turbinates, where this epithelial type is mostly seen (Fig. 2.16). Depending on the severity and duration of exposure, ongoing regenerative hyperplasia may be present if a population of basal cells is preserved. Olfactory epithelial alterations due to systemic absorption and localised metabolism of the test article also are seen in noninhalation studies, such as with 3-methylindole in mice when administered orally. Local levels of metabolic enzymes within the epithelium govern the distribution of lesions [18]. Methimazole in Long-Evans rats, when administered either orally or intraperitoneally, produces damage to sustentacular and sensory cells while sparing basal cells and the basement membrane [19].

In rodents, lesions of the caudal nasal turbinates also occur in oral gavage studies, as a result of aspiration during dosing or gastric reflux. Findings in the turbinates include proteinaceous fluid or inflammatory exudate

in the lumen. Acute necrosis and desquamation of the olfactory epithelium lining the ethmoid turbinates typically are present, sometimes accompanied by inflammatory and degenerative changes of the respiratory epithelium. Changes in the nasopharynx sometimes are present, indicating the pathogenesis of the lesion (Figs. 2.17 and 2.18).

Gastric reflux is a multifactorial phenomenon in rodents, and factors include the animal's size, age, fasting status and the volume administered. Test materials that affect peristalsis or delay gastric emptying, such as antimuscarinics and  $\beta$ -adrenergics, or that display physicochemical properties such as high viscosity, also may predispose to reflux [20].

Tumours of the nasal turbinates have been induced by several classes of compounds administered by systemic or inhalation routes. Nitrosamines cause papillomas and squamous cell carcinomas in rats when given subcutaneously (Fig. 2.19). Dioxane in the drinking water induces papillomas and carcinomas in rats. Formalin administered by inhalation produces squamous cell carcinomas in rats and mice [21]. Olfactory neuroblastomas are rarer but may be induced by genotoxic carcinogens [22] and also by phosphodiesterase (PDE)-4 inhibitors.

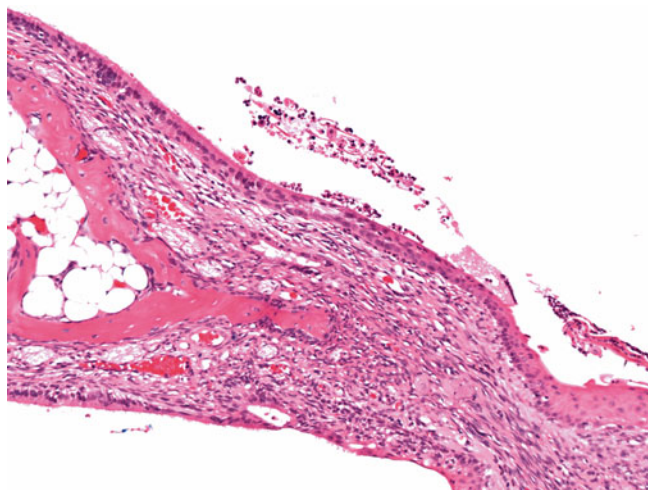


**FIGURE 2-15.** Respiratory and squamous metaplasia in the nasal turbinates of a rat given a muscarinic antagonist. The olfactory epithelium (*left*) has been partially replaced by a more ciliated cuboidal respiratory epithelium adjacent to it and by squamous epithelium further towards the *right*. Inflammatory cell debris, fibrin, and keratin are present in the lumen. H&E.

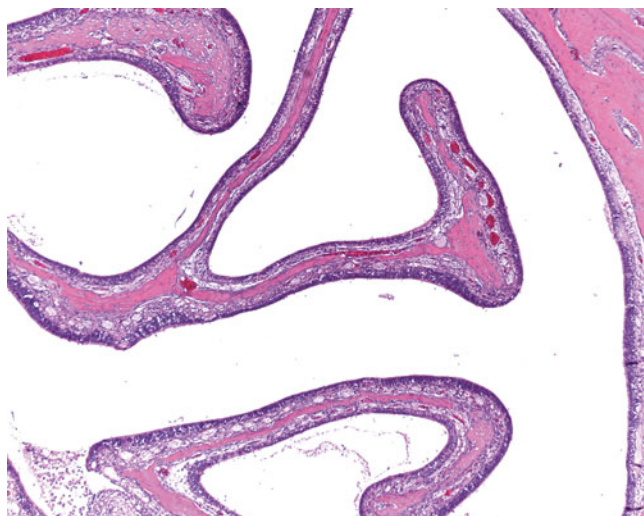


**FIGURE 2-16.** Diffuse olfactory epithelial atrophy of the nasal turbinates in a rat given an industrial chemical. The olfactory epithelium along the dorsal meatus and turbinates appears unevenly thinner, with cell loss and/or disorganisation in many areas. H&E.



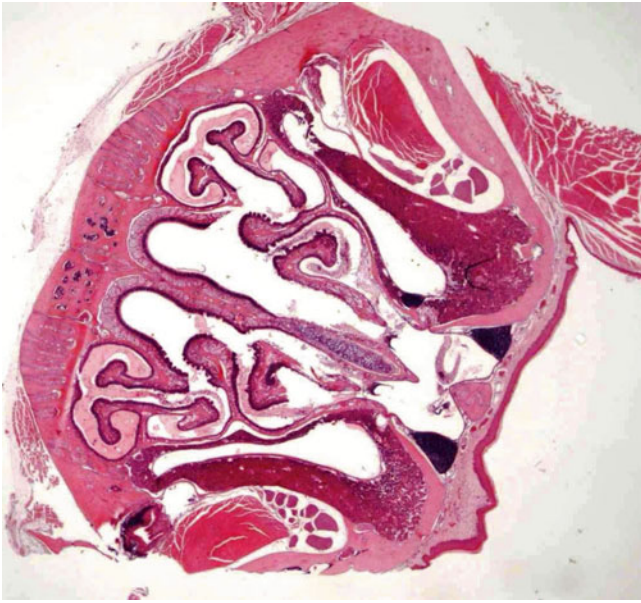


**FIGURE 2-17.** Reflux-associated changes in the nasal turbinates of a mouse given a pharmaceutical by gavage. Eosinophilic fluid containing inflammatory cells is seen in the dorsolateral aspects of the nasal cavity, between the ethmoid turbinates. Exudate in the nasopharynx indicates the likely pathogenesis. These are the areas often affected in reflux. Volume of dose, increased gastric transit time, and pharmaceutical effects may all be involved in this phenomenon. H&E.

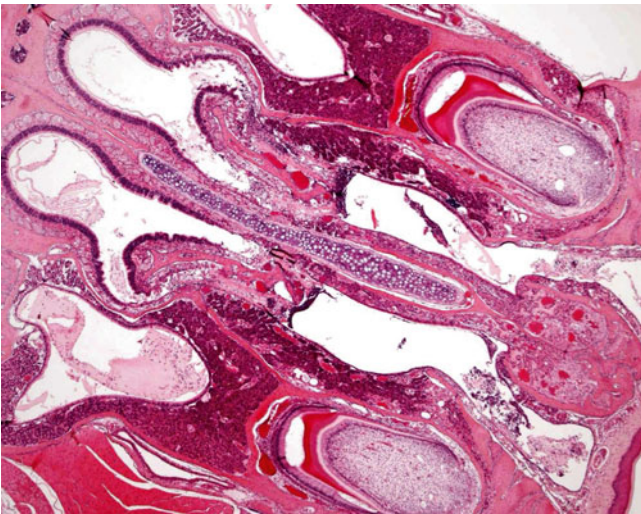


**FIGURE 2-18.** Reflux-associated changes in the nasal turbinates of a mouse given a pharmaceutical by gavage. Eosinophilic fluid and inflammatory debris are seen in the lumen. Fibrinous adhesions are developing between the lateral walls, turbinates, and middle septum. H&E.

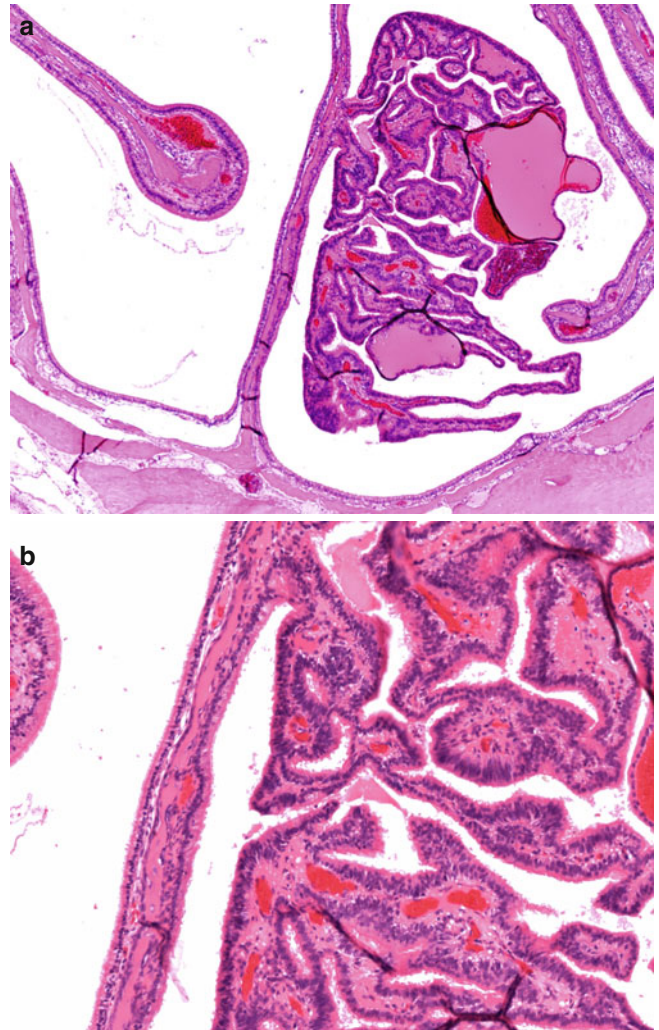


**FIGURE 2-19. (a, b)** Papilloma in the nasal turbinates of a mouse. A well-circumscribed papillary proliferation, with a few dilated glandular structures containing eosinophilic fluid, is present between the turbinates. Columnar epithelium covering the papillary projections is well differentiated. H&E.

## 2.3 Pharynx

Although the pharynx and nasopharynx are examined regularly in inhalation studies, induced changes are rare. In dogs and primates, the pharyngeal tonsils and other respiratory-associated lymphoid tissues often reflect stimulatory or depressive effects on the immune system. Inhaled and oral steroids cause immunosuppression and lymphoid depletion. Toll-like receptor inhibitors are associated with germinal centre devel-

opment because of their immunostimulatory effect (Fig. 2.20).

Eosinophilic droplets in the respiratory epithelium of the pharynx have been recorded with mildly irritant compounds, including neurokinin receptor antagonists.  $\beta$ -adrenergics may cause epithelial degeneration in the pharynx (Fig. 2.21), with the normal respiratory epithelium being replaced by flattened regenerating epithelium.

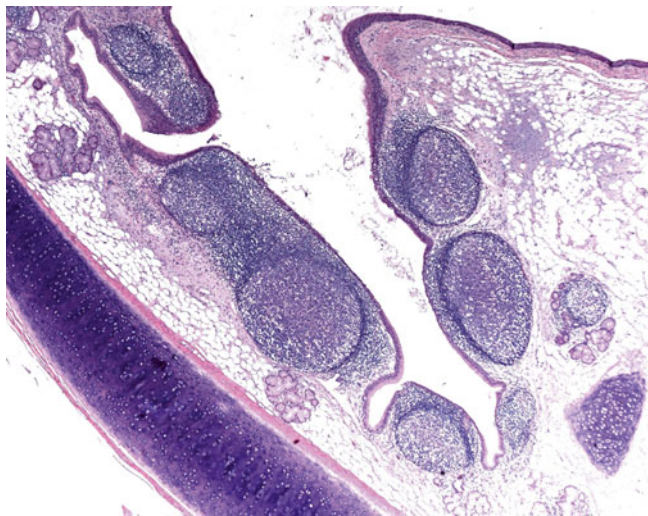


**FIGURE 2-20.** Lymphoid hyperplasia of the pharynx from a cynomolgus monkey treated with an inhaled immunostimulant. The tonsils display large active germinal centres within the lymphoid follicles. H&E.

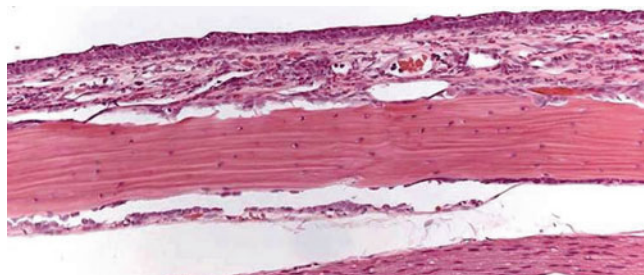


**FIGURE 2-21.** Regenerating epithelium in the pharynx of a rat given an irritant inhaled compound. The normal ciliated respiratory epithelium has been replaced by flattened regenerating basophilic epithelial cells, with a loss of goblet cells. H&E.



## 2.4 Larynx

The larynx is a well-recognised site of induced toxicity in rodent inhalation studies, in which it is particularly susceptible to even minimal irritant effects. Several schemes for sectioning and examining the rodent larynx are followed in different laboratories, with 3–11 sections generally being examined. It is essential that the predilection sites for toxicologic changes are examined consistently and that the pathologist is familiar with the structure of different areas of the larynx [23–25]. These areas are the inner aspects of the arytenoid cartilage, the laryngeal mucosa rostral and lateral to the ventral pouch, and the ventrolateral region at the base of the epiglottis, which is a transitional zone between the squamous and respiratory epithelium.

Exposure to a range of chemicals and pharmaceuticals is associated with changes in the larynx. Pharmaceuticals include  $\beta$ -adrenergics, p38 inhibitors, muscarinic antagonists, and many other compound classes. Changes seen in the larynx are mostly in the epithelium and are as follows:

- Inflammation, degeneration, and necrosis
- Erosion and ulceration
- Squamous metaplasia
- Cartilage necrosis
- Hyperplasia and neoplasia

The larynx's responses to insult are limited and non-specific. The most frequently observed change in the rodent is squamous metaplasia, generally seen first in the ventral aspect of the larynx at the base of the epiglottis [23]. This change may manifest as soon as within 3 days of exposure [24]. Often there is little or no inflammatory response associated with this change. Dilation with degeneration and atrophy of the submucosal glands at the base of the epiglottis is seen less

commonly. This arises as a result of inflammation and erosion and/or squamous metaplasia of the respiratory epithelium, resulting in the sealing off of the ductal opening and leading to acinar cystic distension and eventually atrophy [24]. Squamous metaplasia of the glands and their ducts also may be a sequel (Fig. 2.22).

If irritation is more marked or prolonged, the lateral aspects of the laryngeal mucosa and the arytenoids also exhibit squamous metaplasia/hyperplasia, sometimes with keratinisation. If recovery is allowed, this finding generally will show partial regression. Squamous metaplasia of the larynx often shows a characteristic lack of progression, even in 2-year studies, and is widely accepted as a rodent-specific adaptive response that is of no relevance to humans [26, 27].

Necrosis of the laryngeal U-shaped cartilage also is associated with low-grade irritation and is thought to be a sequel to initial ulceration of the ventral epithelium, followed by necrosis of the underlying cartilage. The epithelium then regenerates and the larynx presents with intact, often metaplastic, epithelium covering an area of necrotic cartilage. The commonest site for cartilaginous necrosis is at the entrance to the ventral pouch, presumably because of its superficial location here [24]. The cartilage appears as a persistent pink homogenous mass with loss of cell detail, with a noticeable lack of inflammation (Fig. 2.23). More rarely, necrosis of the arytenoid cartilage may occur.

Repair of necrotic cartilage, which may occur depending on the extent of damage, manifests as regenerating cartilage from the intact portion, which appears around, but not within, the necrotic area. The new cartilage appears as foci of basophilic chondrocytes around the margins of the necrotic tissue (Fig. 2.24).

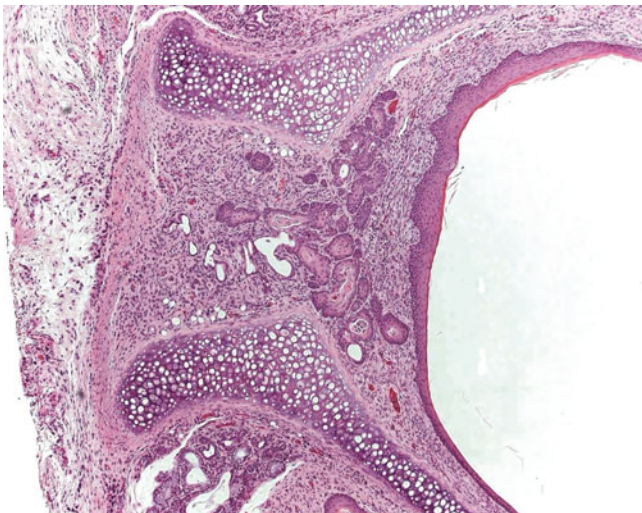


**FIGURE 2-22.** Squamous metaplasia in the larynx of a rat given an irritant inhaled pharmaceutical. The underlying mucous glands and their ducts also show squamous metaplasia. The submucosa is mildly inflamed, with cellular debris present within the ducts and acini. This site is a common target for irritant compounds in rodent inhalation studies. H&E.

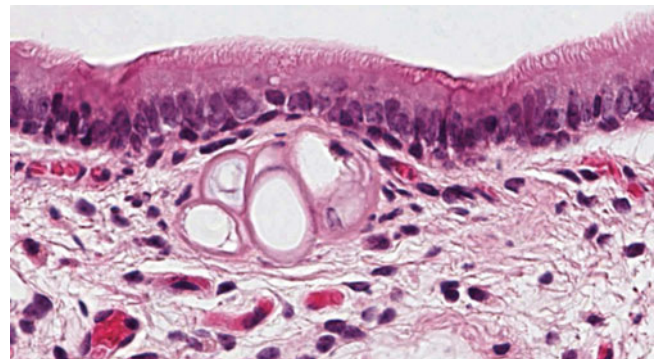


**FIGURE 2-23.** Necrosis of the U-shaped cartilage in the larynx of a mouse given a  $\beta$ -adrenergic agent. The necrotic cartilage appears as a pink homogenous mass, preserving its outline although cellular detail is lost. Necrotic cartilage persists for a very long period. H&E.

Benign and malignant squamous epithelial neoplasms have been induced in rodent larynges by intratracheal instillation of polycyclic aromatic hydrocarbons.

Induced lesions of the larynx in dogs and monkeys are rare. Irritant compounds sometimes induce varying degrees of inflammatory cell infiltrate and, rarely,

erosion and ulceration of the laryngeal epithelium. Occasionally, as a spontaneous finding, focal ulceration with inflammation and necrosis is seen on the vocal folds in dogs, near the junction of the lateral ventricles with the laryngeal lumen. These lesions often are bilateral.

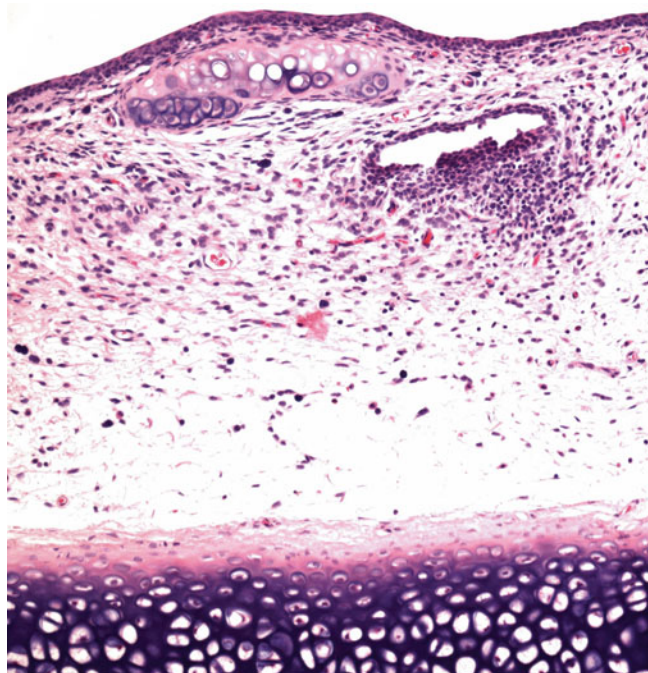


**FIGURE 2-24.** Cartilage necrosis and regeneration of the larynx from a rat given a muscarinic antagonist. The main portion of the cartilage is pink and necrotic with loss of cellular detail, but some basophilic areas of healthy cartilage are present at the periphery, possibly indicating regeneration. H&E.



## 2.5 Trachea/Tracheal Bifurcation

Treatment-related findings in the upper trachea include the following:

- Loss of cilia with flattening of epithelium
- Epithelial vacuolation
- Inflammation/disorganisation/regeneration
- Degeneration and necrosis
- Erosion and ulceration
- Hyperplasia and neoplasia
- Squamous metaplasia

In reality, however, the trachea rarely displays induced changes. In gavage studies, erosion or degeneration, often with regeneration, of the tracheal epithelium sometimes is seen as the result of small quantities of the test article entering the trachea during the dosing procedure or as a result of reflux. Inflammation with epithelial disorganisation and regeneration has been seen with an inhaled industrial chemical in our laboratory (Fig. 2.25). Vacuolation of the tracheal epithelium is sometimes seen as part of a generalised phospholipidosis.

Unlike the trachea, the carina at the tracheal bifurcation is a common target site for changes in

inhalation studies. This is a result of flow dynamics in the upper airways during inhalation, leading to impaction of particles at this site. Changes seen here include loss of cilia; degeneration, disorganisation, and regeneration of the respiratory epithelium at this site; and squamous metaplasia. Loss of cilia appears as a flattening and a basophilic appearance of the epithelial cells at the tip of the carina, with cilia being absent or sparse (Fig. 2.26). Squamous metaplasia is diagnosed when there are several layers of flattened epithelial cells covered by the umbrella cells typical of squamous epithelium (Fig. 2.27). These changes are nonspecific, and their severity depends on the irritancy of the compound, the length of the exposure, the nature of the test article, and other factors. Induced changes are seen with muscarinics,  $\beta$ -adrenergics, and chemicals, including tobacco smoke. Artefactual flattening of the epithelium and erosion are common because of the delicacy of the carina and should be distinguished from genuine induced changes.

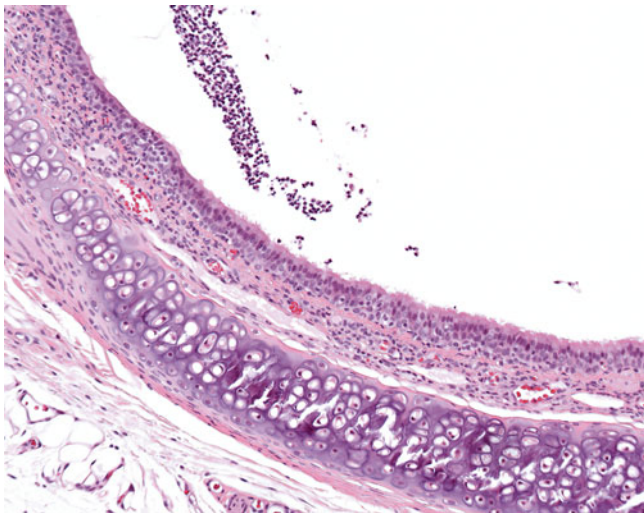


**FIGURE 2-25.** Inflammation of the trachea from a rat given an industrial chemical by inhalation. The tracheal epithelium is disorganised and mildly hyperplastic, with degenerating cells, inflammation, and focal loss of cilia. Neutrophils are present in the lamina propria and lumen. H&E.



**FIGURE 2-26.** Loss of cilia in the carina of a rat given an irritant inhaled compound. The tip of the carina shows flattening and basophilia of the epithelial cells, with focal loss of cilia. This is a common site for changes in rodent inhalation studies because of particle impaction at this point. H&E.

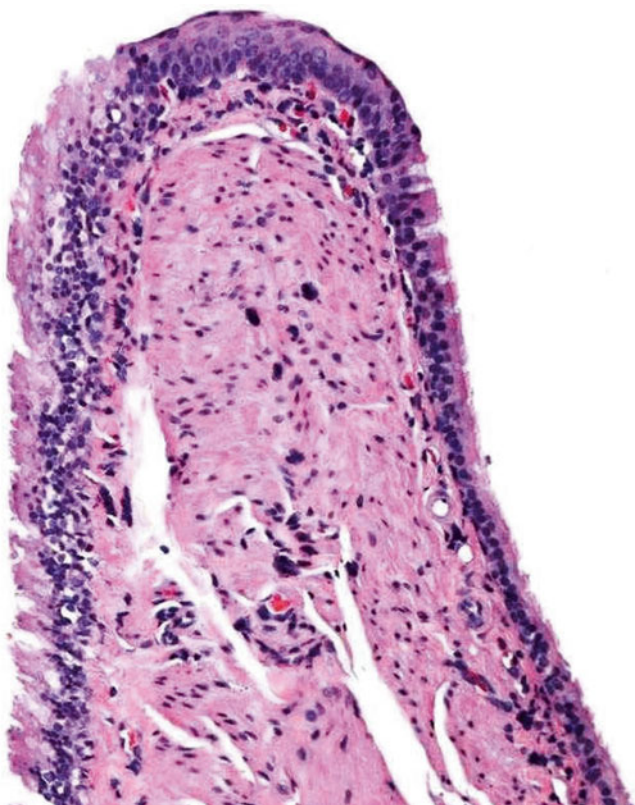


**FIGURE 2-27.** Squamous metaplasia of the carina from a rat given a muscarinic antagonist. The respiratory epithelium at the tip of the carina has been replaced by stratified squamous epithelium, with characteristic cells. H&E.

## 2.6 Bronchi/Bronchioles

The bronchioles are lined by respiratory epithelium. Epithelial regeneration takes place through the Clara cells, the numbers of which increase with penetration into the lung and are greatest in the terminal bronchioles. Changes in the bronchioles include those typical of respiratory epithelia, along with some more specific changes:

- Clara cells—eosinophilic inclusions
- Mineralisation
- Goblet cell hyperplasia
- Degeneration and necrosis
- Erosion and ulceration
- Hyperplasia and neoplasia
- Squamous metaplasia
- Neuroendocrine cell proliferation

Eosinophilic inclusions may occur as an induced change in the bronchiolar epithelium. Although they also are seen as a background finding, their incidence and severity are exacerbated by a variety of inhaled substances. No widely accepted mechanisms have been described for this change. Large spherical eosinophilic inclusions in the Clara cells are induced by inhaled steroids and steroid receptor agonists (Fig. 2.28). These inclusions have been found to be strongly positive for surfactant protein-D and weakly positive for Clara cell secretory protein [28].

Mineralisation of the bronchiolar epithelium is caused by vitamin D analogues in rats. The bronchiolar

epithelial cells and subepithelial collagen contain dark purplish concretions with little or no inflammatory cell reaction (Fig. 2.29).

Low levels of irritation, as seen with gases such as sulphur dioxide, tobacco smoke, and pharmaceuticals, including  $\beta$ -agonists, cause increases in the size and number of mucin-secreting cells, giving the epithelium a hypertrophic appearance (Fig. 2.30). Goblet cells may extend further down the airways than normal, and mucus may accumulate in the airways or alveoli. This finding generally shows complete reversal once the source of irritation is removed. Systemic injections of isoprenaline and pilocarpine also induce changes in goblet cell numbers [29].

A wide range of pharmaceutical classes, chemicals, and gases induce inflammatory and degenerative changes in the bronchiolar epithelium, including tyrosine kinase inhibitors and Toll-like receptor agonists. These changes include peribronchiolar and bronchiolar epithelial inflammation, Clara cell degeneration, and focal or diffuse erosion and ulceration of the bronchiolar epithelium (Fig. 2.31). Varying degrees of inflammatory exudate containing mucus, degenerating inflammatory cells, and other debris sometimes are present in the lumen (Fig. 2.32). Degenerating or ulcerated epithelium may be replaced by regenerating bronchiolar epithelium or may undergo squamous metaplasia (Fig. 2.33).



Neuroendocrine cell hyperplasia occurs spontaneously as a background change in rodents, but physiological conditions such as chronic hyperoxia and pulmonary hypertension cause increases in numbers of neuroendocrine bodies, pulmonary neuroendocrine (PNEC) hyperplasia, or both, in rats. These bodies appear as groups of tightly packed nonciliated cuboidal, oval, columnar, or round cells containing argyrophilic granules, which are positive for corticotropin, calcitonin gene-related peptide (CGRP), and neuron-specific

enolase. The cells have round basophilic nuclei and scant cytoplasm, closely resembling lymphocytes, and require immunohistochemical staining for confirmation (Fig. 2.34). Ultrastructurally, dense-core cytoplasmic granules of the amine-precursor uptake decarboxylase type may be seen. Silica induces hyperplasia of rat alveolar neuroendocrine bodies but not bronchiolar neuroendocrine bodies [30]. Exposure of hamsters to chemical carcinogens such as nitrosamines often leads to marked but reversible PNEC hyperplasia [31].

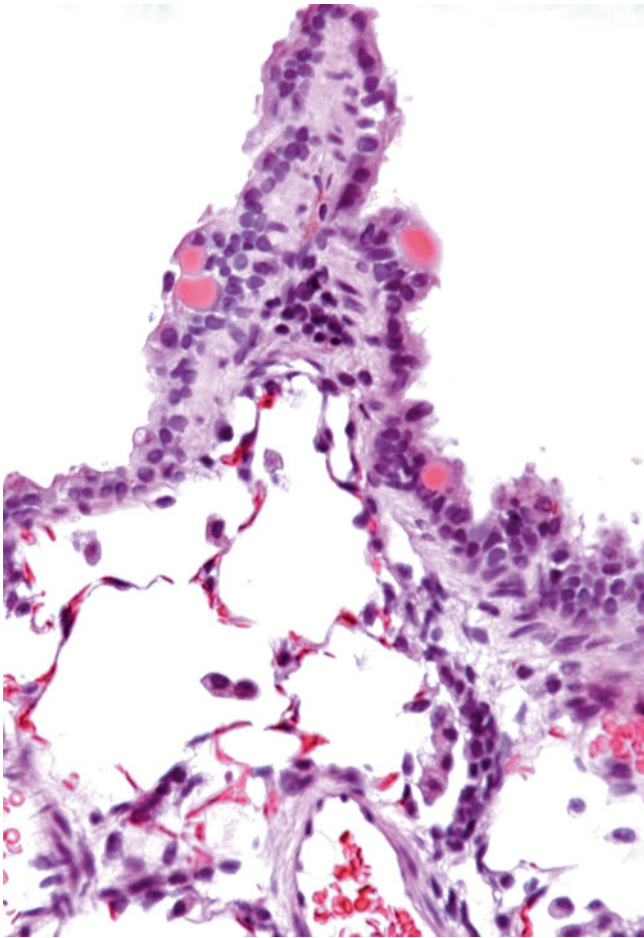


**FIGURE 2-28.** Eosinophilic inclusions in a bronchiole from a rat treated with a steroid in a long-term study. Large spherical eosinophilic inclusions are present in some of the Clara cells. These inclusions consist of surfactant and secretory proteins. H&E.

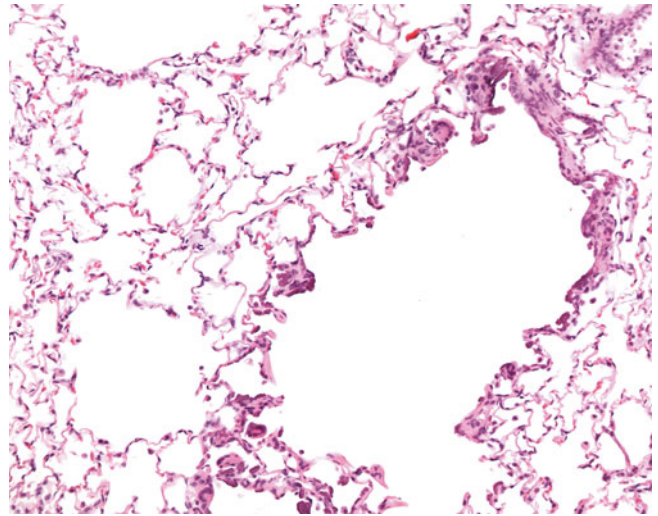


**FIGURE 2-29.** Mineralisation of the bronchiolar epithelium in a rat given a vitamin D analogue. Dark purplish concretions are seen within the bronchiolar epithelial cells and sometimes within the underlying collagen. H&E.

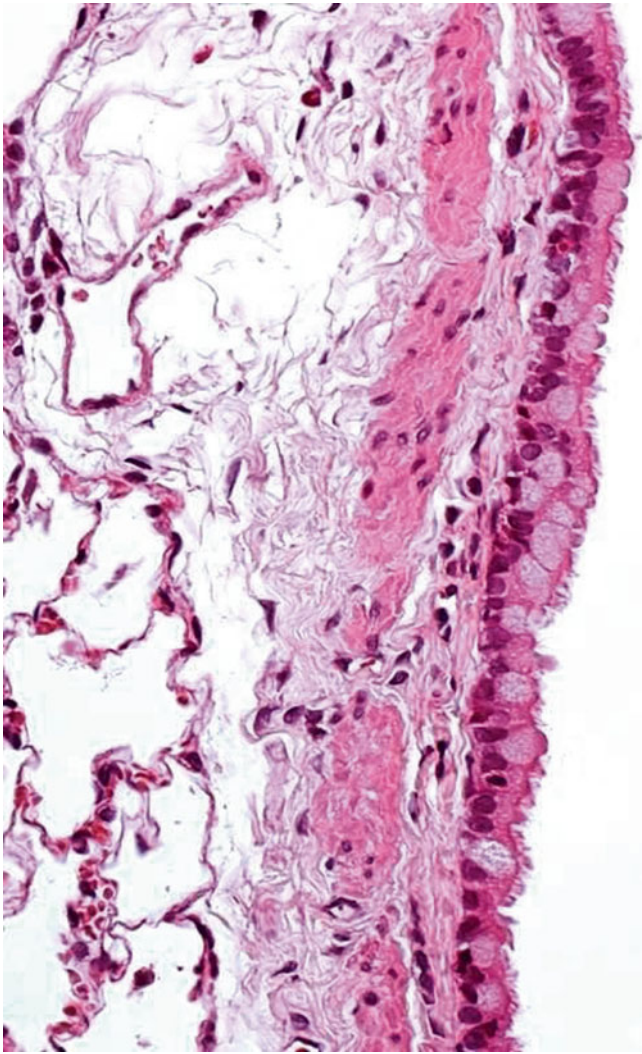


**FIGURE 2-30.** Goblet cell hypertrophy/hyperplasia of the terminal bronchiole in a rat. This is characterised by an increase in the size and number of goblet cells. The respiratory epithelium consists largely of mucus-producing goblet cells, which have replaced the normal varied epithelial population. H&E.

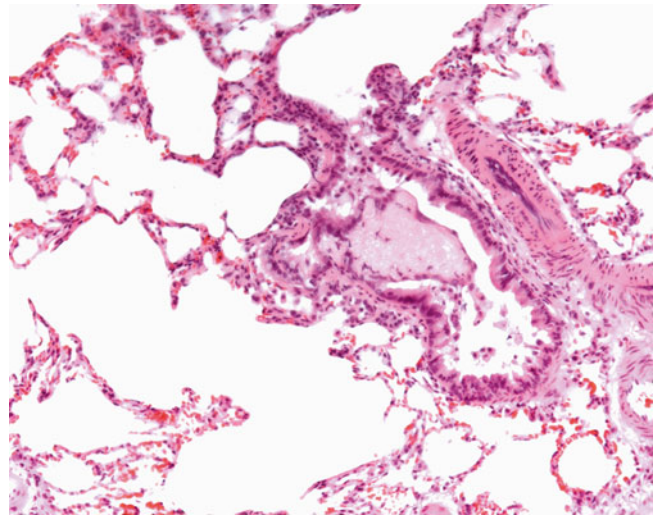


**FIGURE 2-31.** Focal inflammation of the terminal bronchiole in a rat that received a biologic. Amorphous debris has accumulated beneath and is elevating the bronchiolar epithelium, causing focal erosion. Inflammatory cell debris is present in the bronchiolar lumen. H&E.

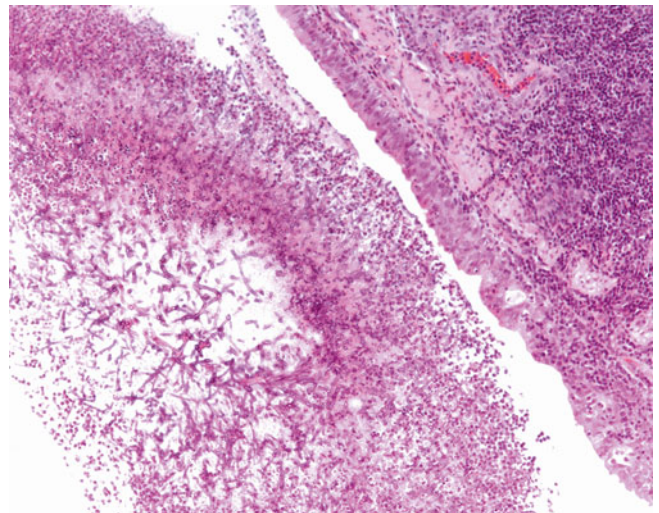


**FIGURE 2-32.** Inflammation in the bronchiole of a rat given a biologic. Exudate comprising degenerating neutrophils and fibrin is present in the airway, with numerous fungal hyphae evident in the exudate. The bronchiolar epithelium is mildly inflamed and hyperplastic. H&E.



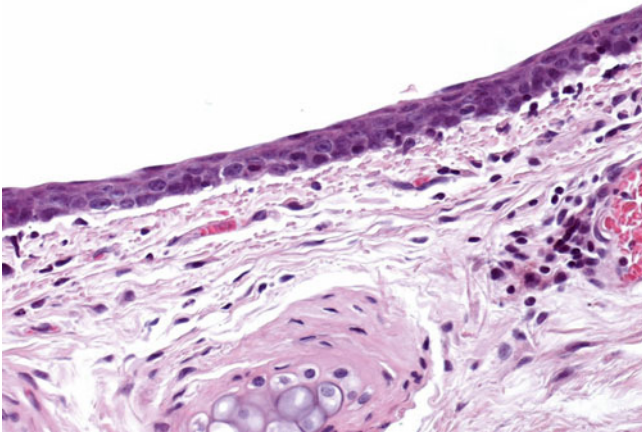


**FIGURE 2-33.** Squamous metaplasia in the bronchus of a rat given an irritant test article. The normal bronchial epithelium has been replaced by mature stratified squamous epithelium. A few lymphocytes are present in the submucosal tissue associated with the area of squamous metaplasia. H&E.

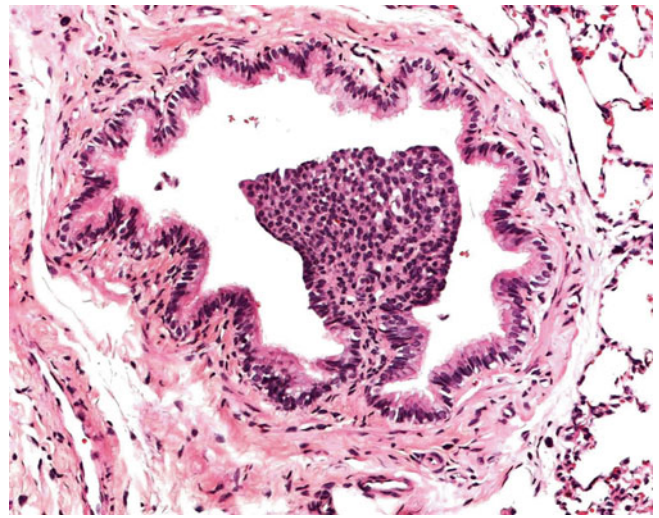


**FIGURE 2-34.** Neuroendocrine cell hyperplasia in the bronchiole of a rat. A polypoid structure composed of round cells with round dark nuclei and scanty cytoplasm protrudes into the bronchiolar lumen. Immunohistochemistry is necessary to differentiate these from similar-appearing lymphoid aggregates. H&E.

## 2.7 Terminal Bronchioles/Alveolar Ducts

In inhalation studies, induced changes commonly are seen in the terminal bronchioles, where the test material is deposited. The nature of the induced changes depends on several factors including particle size, the nature of the test material, and its pharmacological action. Because this area contains both airways lined by respiratory epithelium and alveoli, toxicologic changes in these regions often involve the cell types of both areas. Changes affecting the terminal bronchioles alone are similar to those described in the previous section. Changes in the alveolar ducts are listed below:

- Increased alveolar macrophages
- Eosinophilic deposits/hyaline membranes
- Epithelialisation/bronchialisation/type II pneumocyte proliferation
- Squamous metaplasia
- Collagenisation/fibroplasia

Oxidant gases (nitrous oxide, oxygen, ozone) tend to affect ciliated cells in the terminal bronchioles more severely, probably because protective mucus is thinner at this site.

Increases in alveolar macrophages reflect an increased nonspecific clearance response to inert

inhaled materials (Fig. 2.35). With more reactive compounds, macrophages may coalesce, forming multinucleate cells or granulomas [32].

Deposition of amorphous eosinophilic material, seen lining the alveolar ducts, occurs in treatment with Toll-like receptor agonists and other agents causing alveolar damage (Fig. 2.36).

At the bronchiolar–alveolar junction, ciliated cuboidal cells may proliferate and extend along the alveolar septae, a process known as bronchialisation (Fig. 2.37). This is a protective adaptation. Bronchialisation often is accompanied by thickening of the alveolar septum and sometimes an inflammatory reaction. Squamous metaplasia of the terminal bronchiolar epithelium also may develop as a protective response to inert particles, sometimes becoming quite extensive (Fig. 2.38).

Perivascular and peribronchiolar collagenisation or fibrosis at the junction is associated with a range of compounds, including industrial chemicals and pharmaceuticals such as PDE-4 inhibitors. Morphologically, varying degrees of subepithelial collagen deposition and/or fibrosis are seen in the alveolar ducts and bronchiolar walls (Fig. 2.39).

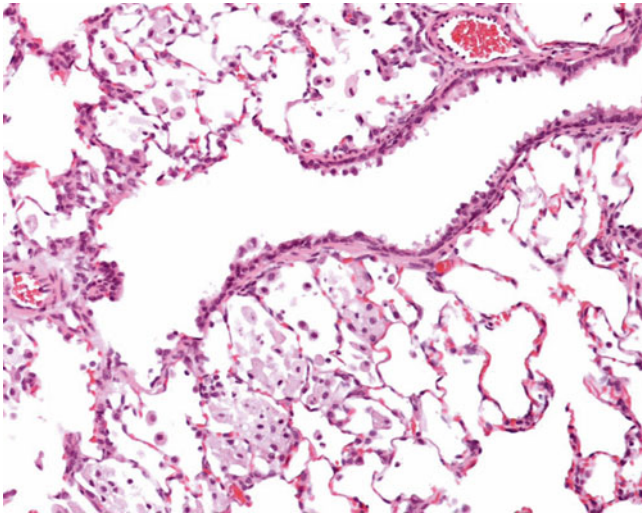


**FIGURE 2-35.** Foamy macrophage aggregates in the lung of a rat. Foamy macrophages are seen in the alveoli surrounding the terminal bronchiole and alveolar duct. This is a characteristic target site in inhalation studies and indicates an increased clearance response to inert inhaled materials. H&E.

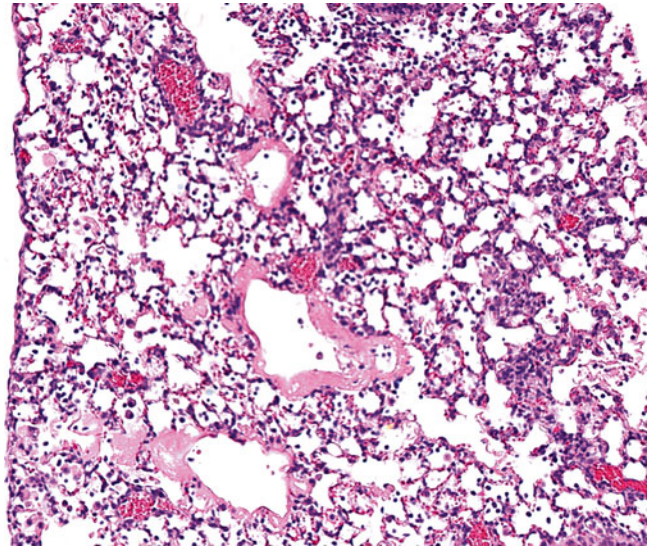


**FIGURE 2-36.** Hyaline membrane formation in the lung of a rat given a biologic. The alveolar ducts are lined by fibrinoid eosinophilic material, with a glassy appearance. Inflammatory cells are present in the alveoli, with focal interstitial inflammation. H&E.

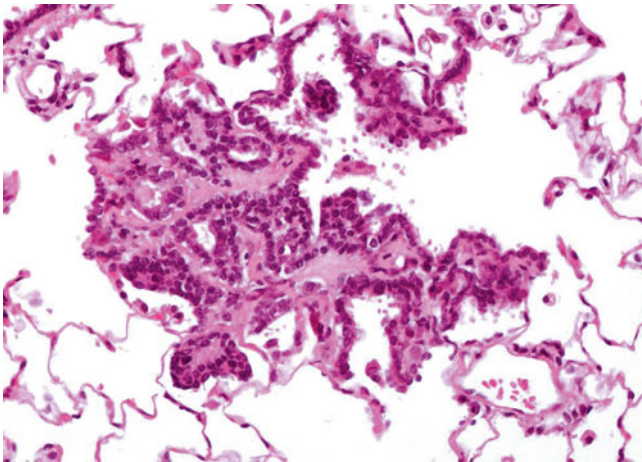


**FIGURE 2-37.** Ciliated cuboidal metaplasia in the lung of a rat. Focal alveoli at the bronchiolar-alveolar junction show septal thickening and are lined on both surfaces by cuboidal ciliated cells. This process also is known as bronchialisation. H&E.

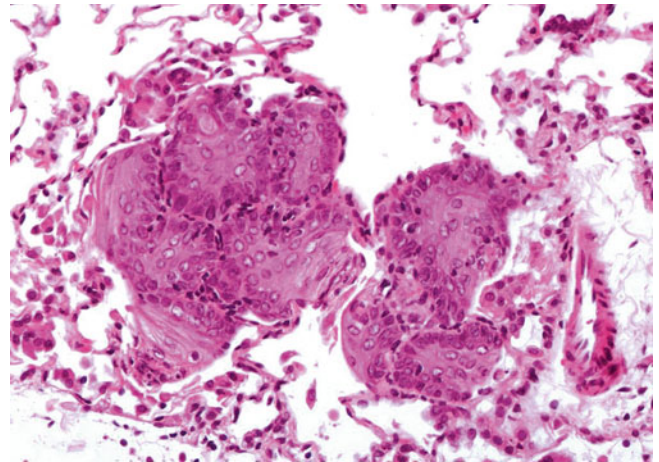


**FIGURE 2-38.** Squamous metaplasia of the bronchiolar-alveolar junction in a rat given a particulate compound. Marked squamous epithelial proliferation has partially occluded the airway, largely replacing the normal respiratory epithelium. This is well-differentiated squamous metaplasia, a protective response. H&E.



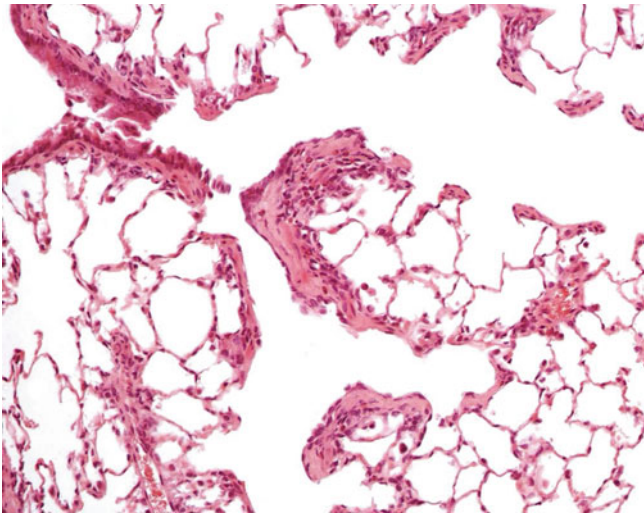


**FIGURE 2-39.** Collagenisation/fibrosis at the bronchiolar–alveolar junctions in a rat treated with a PDE inhibitor. Localised subepithelial collagen deposition with minimal fibrosis is present in the bronchiolar and alveolar duct walls. H&E.

## 2.8 Lungs

Pathologic changes in the lung generally result from an overload of clearance mechanisms, direct toxicity, and indirect toxicity due to metabolic activation or immune-mediated effects. They include:

- Increased alveolar macrophages, lipidoses, phospholipidoses, lipoproteinosis
- Epithelialisation—type II pneumocyte proliferation
- Alveolar mineralisation
- Alveolitis
- Alveolar injury—oedema, haemorrhage, necrosis, fibrosis
- Inflammation/thickening/pneumonitis/pneumonia
- Bronchiolar-associated lymphoid tissue hyperplasia/depletion
- Vascular/pleural changes
- Bronchioloalveolar hyperplasia
- Bronchioloalveolar adenoma/carcinomas
- Squamous metaplasia/epithelial cysts/keratinising epithelioma/squamous cell carcinoma
- Mesothelioma

Increases in the number or nature of alveolar macrophages are a common induced change in inhalation studies and indicate increased clearance of exogenous or endogenous substances. Macrophages may be localised to the alveoli near the alveolar ducts or diffusely distributed. They may contain a variety of substances, including test material, surfactant lipid, phospholipid, blood degradation products, pigments, and others (Fig. 2.40).

Foamy macrophage accumulation frequently is accompanied by alveolar inflammatory cells and thickening of the alveolar wall with inflammatory cells, type II pneumocyte proliferation, and slight increases in reticulin and collagen fibres (Fig. 2.41). Macrophages often form aggregates or granulomas composed of tightly packed and/or coalescing macrophages (Fig. 2.42). Cholesterol clefts often are seen within these granulomas, which may be induced by a variety of inhaled xenobiotics, including dusts, and also occur in systemic lipidosis (Fig. 2.43). Intravenously administered compounds, such

as insoluble polysaccharides, induce localised angio-centric granulomas with epithelioid and foreign-body type giant cells. Procedure-related foreign-body granulomas containing exogenous and endogenous materials, such as fibres, fragments of epithelium, and adipocytes, are seen in intravenous injection and infusion studies (Fig. 2.44). Subcutaneous injection of vegetable oil as a vehicle can also result in lipid-containing macrophage accumulations and lipid granulomas in the lungs (Fig. 2.45).

Several conditions, discussed in the following text, result in a similar histopathological picture with aggregates or diffuse foamy macrophage infiltration. Overloading of macrophages results in rupture, with release of their contents into the alveoli and an associated inflammatory cell reaction.

Phospholipidosis manifests as diffuse or multifocal accumulations of foamy macrophages with secondary features, including eosinophilic alveolar material, type II pneumocyte proliferation, and infiltration with polymorphonuclear cells (Fig. 2.46). On transmission electron microscopy, macrophages contain electron-dense multilamellar bodies, which also are present in type II pneumocytes and Clara cells, as well as in circulating lymphocytes (Fig. 2.47). This condition typically is associated with cationic amphophilic compounds (CADs), such as amiodarone and chlorpheniramine. Species and tissue specificities vary with these drugs. Very few drugs that produce phospholipidosis in rodents are capable of inducing significant phospholipidosis in humans, although amiodarone does induce the condition in rats and humans.

Lipoproteinosis is associated with exposure to dust, such as quartz, and refers to the accumulation of fine, eosinophilic PAS-positive material in the alveoli with increased numbers of large rounded foamy macrophages, which may rupture releasing lipoprotein. Secondary changes include type II pneumocyte proliferation and infiltration with polymorphonuclear cells. Electron microscopy shows that the material is

composed predominantly of lamellar bodies consisting of surfactant from type II cells (Fig. 2.48).

Interstitial pneumonitis with lipid-laden macrophages occurs in rats fed a diet supplemented with cholesterol and cottonseed oil. Initially, macrophages accumulate in the alveoli, but later they may be seen in the subpleural, peribronchiolar, and perivascular regions. This is basically a hyperlipidaemia and also is seen with hypophysectomy and anorectic drugs, both of which reduce food intake and presumably cause hyperlipidaemia.

Mineralisation of the alveolar septae is induced by vitamin D analogues (Fig. 2.49). Dark bluish purple concretions are seen within the alveolar septae.

Inflammatory cell infiltration, septal thickening with collagen, and alveolar macrophages sometimes are associated with these depositions.

Toxicity in the lungs may involve one or more areas, depending on the affected cell type(s). Type 1 pneumocytes and endothelial cells are targets for oxygen toxicity, which has implications for its therapeutic use in premature infants and adults with respiratory distress. Many agents produce respiratory injury by direct interaction of the reactive molecule with the target cells, causing cytolytic changes. Pulmonary toxicity also may be partially mediated through the release of certain proteins; for example, necrosis of the airway epithelium in ozone toxicity is associated with increased levels of

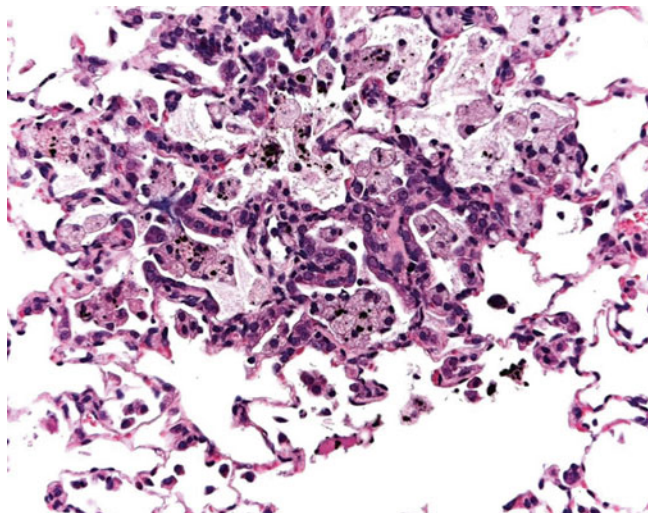


**FIGURE 2-40.** Focal pigmented macrophages containing variably sized black pigment granules in the lung of a rat given a black particulate material. The macrophages, some of which are ruptured, form aggregates. The alveolar septum displays type II pneumocyte proliferation. H&E.

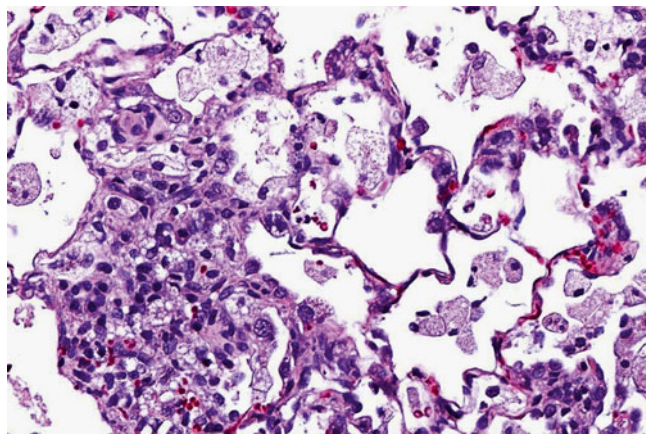


**FIGURE 2-41.** Foamy macrophages with type II pneumocyte proliferation in a rat lung. Large foamy macrophages are present in the alveoli; some of them have ruptured, releasing their contents. Some have coalesced to form an aggregate, and the alveolar septae show focal type II pneumocyte proliferation. H&E.

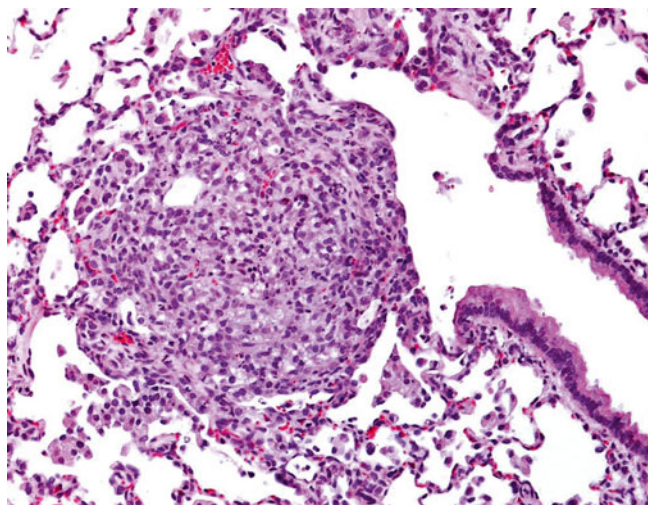


**FIGURE 2-42.** A large granuloma at the bronchiolar-alveolar junction in a rat lung. The granuloma comprises tightly packed large foamy macrophages with a few scattered neutrophils and lymphocytes. H&E.

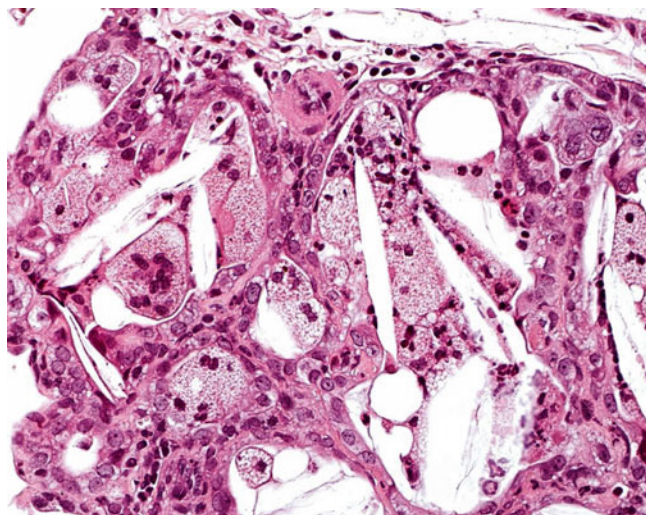


**FIGURE 2-43.** Cholesterol clefts in the lung of a rat with hyperlipidosis. A lesion consisting of coalescing large foamy macrophages is seen. Multinucleate cells, numerous cholesterol clefts, and small numbers of lymphocytes are present. H&E.



CGRP and activation of CGRP receptors and with neurokinin-1 receptor activation [33, 34].

Metabolic activation may occur either in the lung or elsewhere in the body with haematogenous transport of metabolites to the lung. If in the lung, it may occur subsequent to inhalation or blood-borne exposure to the test article. Many pulmonary toxicants are activated as a result of metabolism in the lung [35], where they generally are metabolised in the Clara cells; examples are 4-ipomeanol, carbon tetrachloride, and 3-methylindole.

Pulmonary oedema may be secondary to changes in other organ systems or may be the result of primary lung toxicity. In pulmonary oedema, the alveoli contain proteinaceous eosinophilic fluid with varying numbers of red and white blood cells, depending on the mechanism of

induction and the inflammatory component (Fig. 2.50). Damage to endothelial cells by different mechanisms, such as their metabolism of  $\alpha$ -naphthylthiourea and phenylthiourea, results in damage to capillaries and venules with marked pulmonary oedema. Administration of interleukin 2 causes 'vascular leak syndrome', characterised clinically by pulmonary oedema, pleural effusions, ascites, and other adverse effects, including pulmonary inflammation.

These effects are the result of cytotoxic vascular damage mediated directly by activated killer cells and cytotoxic T lymphocytes, with secondary release of inflammatory cytokines [36]. Many drugs produce pulmonary oedema in humans, either directly or through poorly understood immunogenic mechanisms.

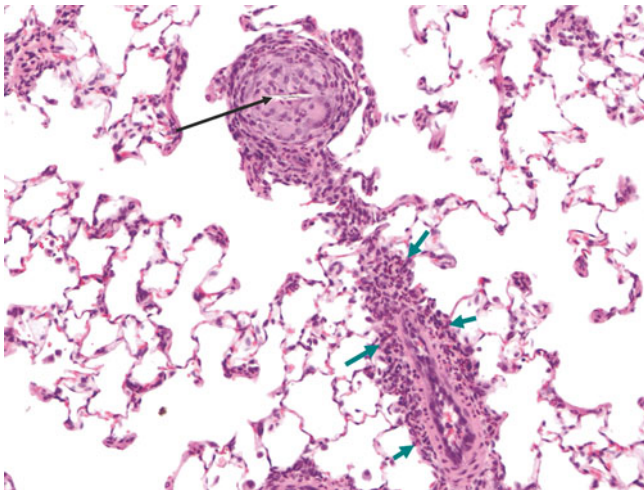


**FIGURE 2-44.** Foreign-body granuloma in the lung of a rat from a continuous intravenous infusion study. The granuloma contains a fibre (black arrow), and the blood vessel shows perivascular inflammatory cell infiltration (green arrows). Both are typical procedure-related lesions in rodent intravenous infusion studies. H&E.

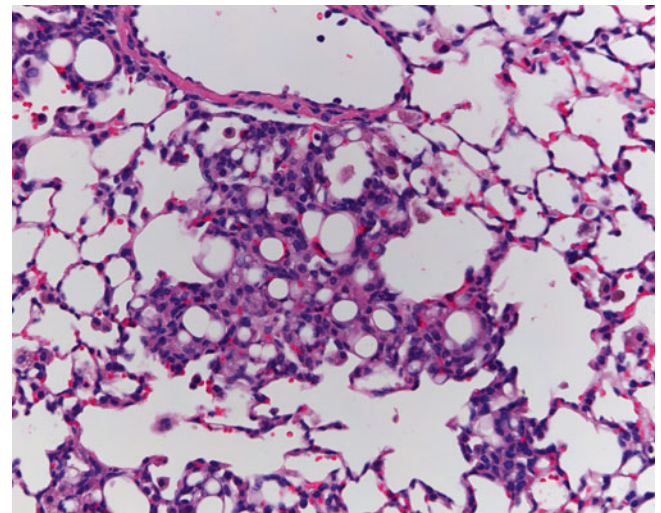


**FIGURE 2-45.** Perivascular/alveolar focus of macrophages containing lipid and pinkish-brown pigment. Large vacuoles resembling lipid are present in some cells. The rat was injected subcutaneously with an oil vehicle. H&E.

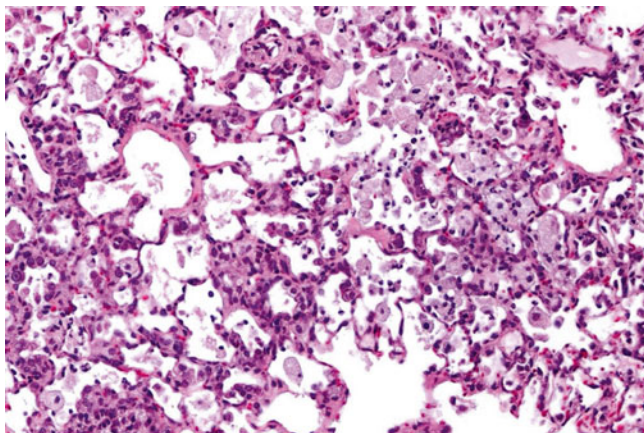


**FIGURE 2-46.** Phospholipidosis in the lung of a rat given a CAD. Diffuse infiltration of alveolar spaces with large foamy degenerating macrophages, as seen in this rat, is characteristic of phospholipidosis. The alveolar septae are markedly thickened with inflammatory cells and collagen, exhibiting type II pneumocyte proliferation. H&E.

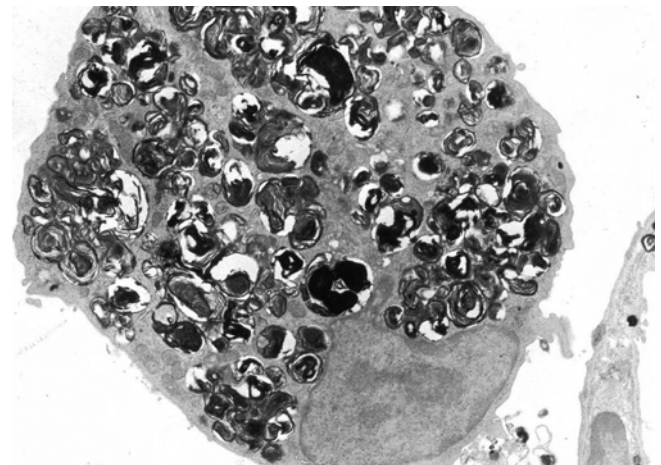


**FIGURE 2-47.** Numerous multilamellar bodies of various sizes and shapes in a pulmonary macrophage from a rat. These bodies are characteristic of phospholipidosis and may be seen in a wide variety of organs (Transmission electron microscopy).



Eosinophilic crystals in the alveoli, often accompanied by macrophages containing red blood cells or pigment, as well as neutrophils, are sequelae of focal haemorrhage (Fig. 2.51). Alveolitis of this type often is seen as a background finding.

Hyaline membranes lining the alveolar ducts are an uncommon response seen with some xenobiotics and strongly positive with PAS staining (Fig. 2.36). Some compounds, including Toll-like receptor agonists, produce a marked inflammatory response, with macrophage

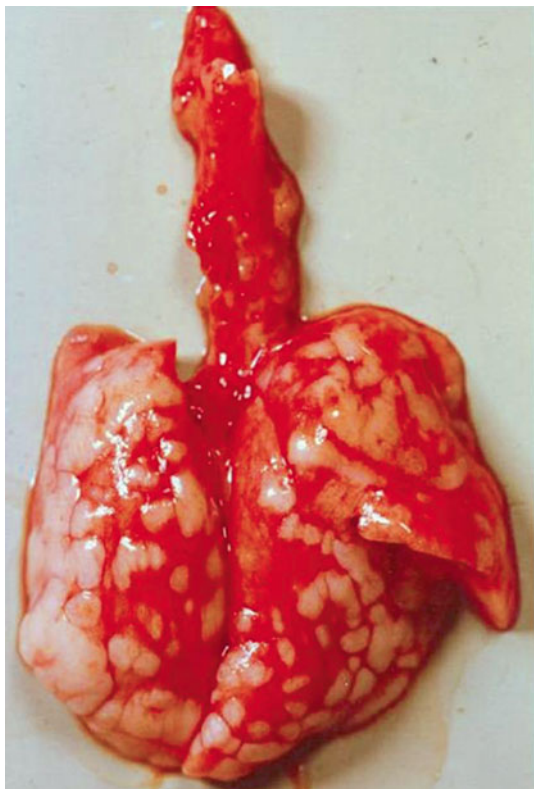


**FIGURE 2-48.** Lipoproteinosis has caused numerous large raised pale coalescing areas on the lungs of this mouse. These correlated histologically with aggregates of foamy macrophages. H&E.

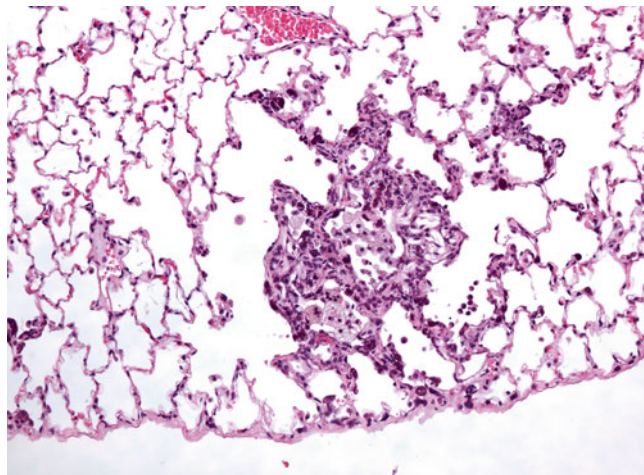


**FIGURE 2-49.** Mineralisation in the lung of this rat was induced by a vitamin D analogue. The change appears as multifocal dark bluish purple concretions in the alveolar septum, which is thickened by inflammatory cells and eosinophilic material. Foamy pigmented macrophage aggregates are present in the alveoli. H&E.

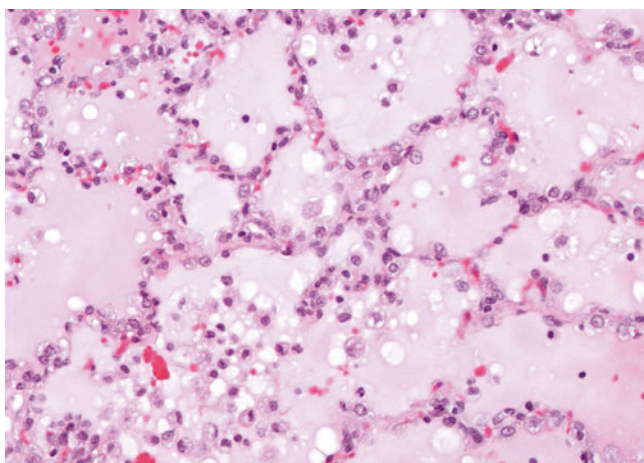


**FIGURE 2-50.** Pulmonary oedema in the lung of a rat. The alveoli are flooded with eosinophilic proteinaceous fluid. Scattered within the fluid are red blood cells and macrophages. The alveolar septum is thickened with intracapillary inflammatory cells in a few areas. H&E.

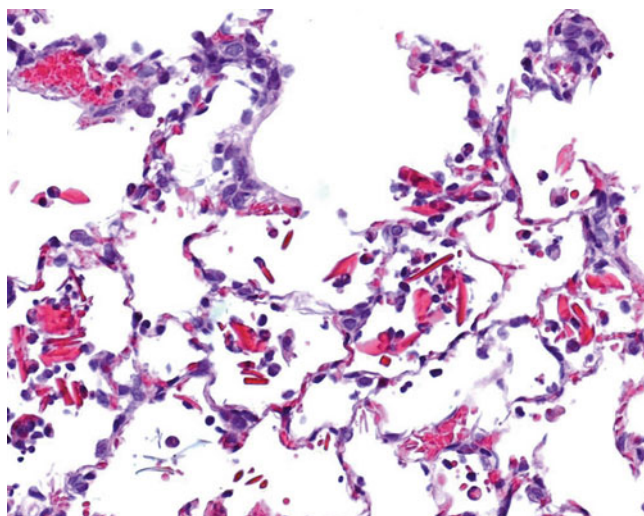


**FIGURE 2-51.** Alveolitis in the lung of a rat. Within the alveoli are several eosinophilic crystals composed of haematoidin. Scattered macrophages containing either pigment or red blood cells also are present. H&E.



aggregates in the alveoli and varying numbers of lymphocytes, plasma cells, and neutrophils within the alveoli and alveolar walls, causing interstitial thickening (Fig. 2.52).

Marked haemorrhage and necrosis of the alveolar walls are induced by paraquat, which selectively targets type I and II alveolar cells because of their possession of a polyamine uptake system. Females are less susceptible to free radical toxicity because of the stimulatory effect of estradiol on antioxidant mechanisms.

Damage to the alveolar walls results in fibrinous exudate and interstitial and alveolar inflammation (Fig. 2.53). If the damage is extensive, alveolar fibrosis develops as a sequel. Antisense oligonucleotides cause

pneumonitis and subsequently alveolar fibrosis. Bleomycin produces interstitial pneumonitis, with extensive fibrosis as a sequel. Because of this effect on the lung parenchyma, it is used to create experimental models of alveolar fibrosis (Figs. 2.54 and 2.55).

Immunosuppression, resulting in impaired defence mechanisms, may result in secondary bacterial and fungal infections. Inhaled corticosteroids cause depletion of the lymphoid tissues associated with the airways (e.g. nasal-associated lymphoid tissue, bronchus-associated lymphoid tissue) (Fig. 2.56), and secondary alveolitis or bronchopneumonia may develop, often localised or confined to one lung lobe.

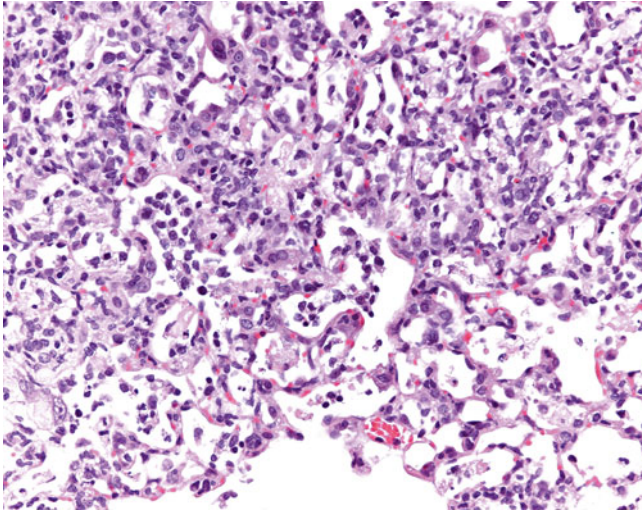


**FIGURE 2-52.** Interstitial inflammation in the lung of a mouse treated with a biologic. Marked interstitial thickening with chronic inflammatory cells and eosinophilic material, probably collagen, is present. Peribronchiolar and perivascular lymphocytic infiltration can be seen. H&E.

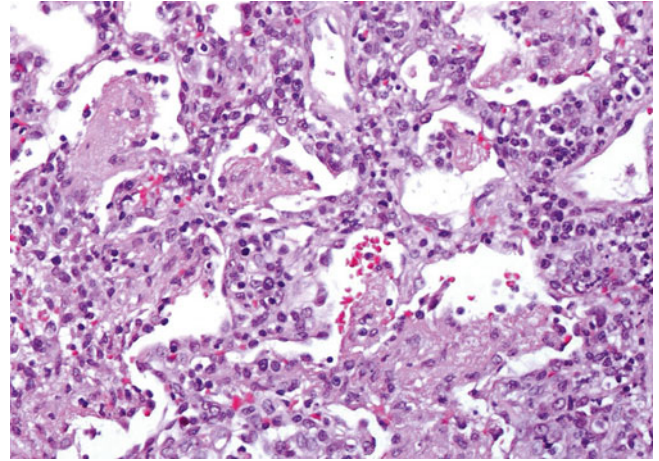


**FIGURE 2-53.** Fibrinous pneumonia in a rat lung. There is marked thickening of the alveolar septae with chronic inflammatory cells. The alveoli contain large amounts of fibrinoid inflammatory exudate, which often adheres to the septae and is starting to undergo fibrosis. H&E.

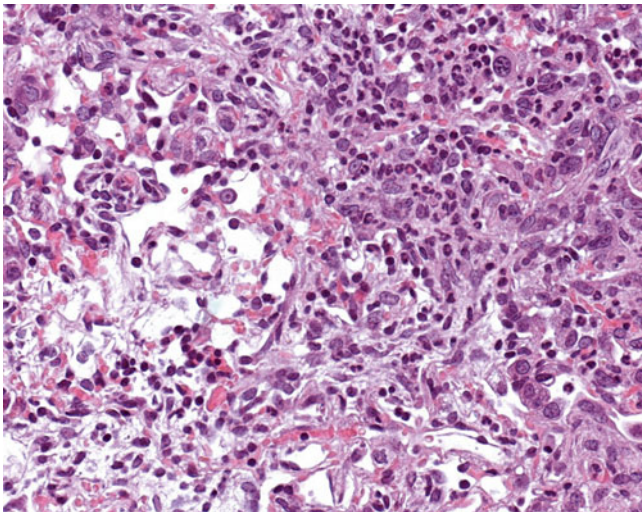


**FIGURE 2-54.** Interstitial pneumonitis and fibrosis in the lung of a rat treated with bleomycin. Mixed inflammatory cell infiltration, type II pneumocyte proliferation, and fibrosis have obscured the normal alveolar architecture. This is typical of bleomycin-induced lung pathology. H&E.

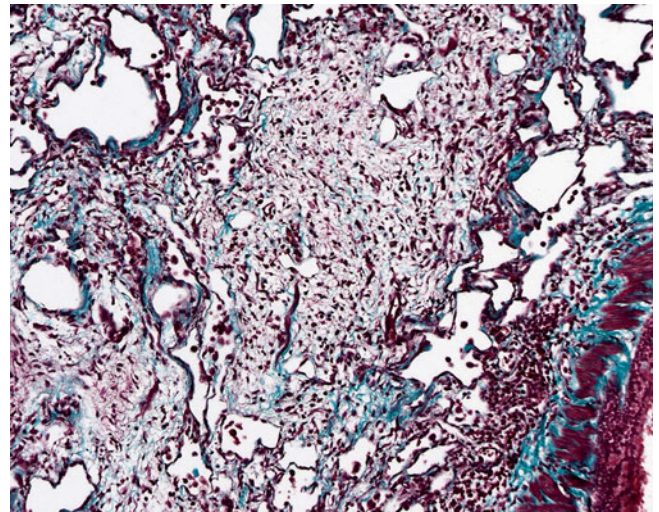


**FIGURE 2-55.** Alveolar fibrosis from the lung of a rat treated with bleomycin. Fibroblasts and collagen appear as a green fibrous matrix that has replaced the normal alveolar septae, with scattered inflammatory cells seen as dark red nuclei. Muscle and epithelia also are stained dark red (Masson's trichrome).



Stimulation of respiratory-associated lymphoid tissue, independent of inflammatory changes in the lungs, has been described in various species with Toll-like receptor agonists, with accompanying stimulation of associated lymph nodes (Fig. 2.57). PDE-4 inhibitors also cause immunostimulation of lymph nodes, partially as a result of inflammatory changes in the lungs.

Overstimulation of immune mechanisms occasionally may result in an adverse effect. The most common hypersensitive responses in the lung are types I and III. In type I, initial exposure results in production of IgE, which binds to mast cells and basophils, resulting in an eosinophil-mediated inflammation. In type III hypersensitivity, repeated exposure results in the development of antibodies and subsequent deposition of antigen-antibody complexes in the lung that fix complement and lead to inflammation. Beryllium has induced a type IV response in dogs, but in rats beryllium merely induces a foreign-body response, as there is no involvement of sensitised T cells in the lesion.

Non-immunologically mediated pulmonary disease may mimic immunologically mediated disease. Certain chemicals stimulate epithelial irritant receptors and cause secretion of inflammatory mediators without antibody involvement, resulting in a pseudoallergic reaction resembling type I hypersensitivity; examples include formaldehyde and ozone.

Misdosing may result in a variety of findings. In rats, oesophageal perforation during gavage can cause deposition of the test article in the thoracic cavity. Pleuritis, pericarditis, perithymic inflammation, and abscess are the common sequelae of intrathoracic dosing. If the article is an irritant, necrosis of the thoracic organs develops, initially involving the surface of the organ.

PDE-4 inhibitors induce pleural inflammation with fibrosis and development of adhesions between lung lobes in rats (Fig. 2.58). Macroscopically, adhesions between lung lobes are seen, with the pleura showing thickening with fibrosis and collagen deposition.

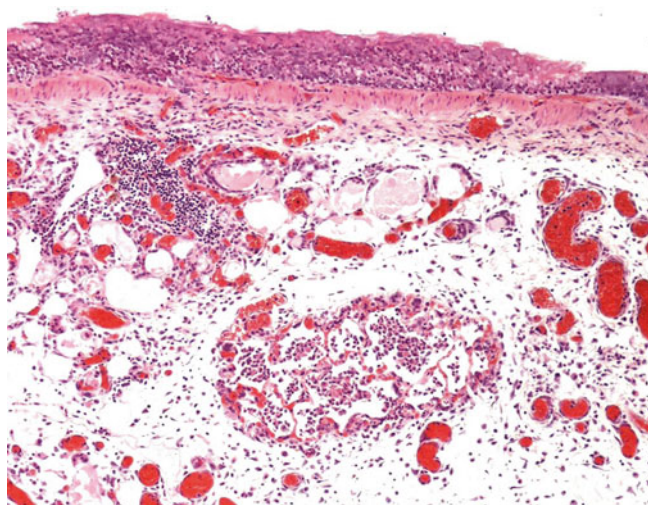


**FIGURE 2-56.** Lymphoid depletion in the lung of a rat given a corticosteroid. The bronchiolar-associated lymphoid tissue shows marked depletion, with a single focus of lymphocytes and a few scattered inflammatory cells remaining. H&E.

Vasculitis of the pulmonary vessels occurs with a variety of vasodilators, including PDE-4 inhibitors. Histologically, varying degrees of perivascular and vascular inflammation and mural necrosis with different proportions of cell types are seen (Fig. 2.59).

Compounds that cause degenerative changes in the myocardium, such as industrial chemicals, may induce similar degenerative findings in intrapulmonary blood vessels that are composed of cardiac muscle. Myofiber vacuolation, degeneration, and inflammatory cell infiltrate have been seen with an inhaled industrial chemical that caused similar lesions in the myocardium (Fig. 2.60).

Hyperplastic and neoplastic lesions in the lungs are induced in rodents by a wide variety of genotoxic and nongenotoxic compound classes administered by inhalation or orally. In mice, surveys have shown that most of these tumours are positive for surfactant apoprotein, indicative of a type II pneumocyte origin [37]. Bronchioloalveolar hyperplasia arises from the alveolar type II cells and/or bronchiolar ciliated respiratory or secretory cells (Fig. 2.61) [8]. This may be classified as alveolar, bronchiolar, or mixed based on cell morphology. When induced, these hyperplasias form a morphological and biological continuum of changes with bronchioloalveolar adenomas and carcinomas. To assess their relationship to the test article and possible carcinogenic potential, all bronchioloalveolar proliferative lesions should be evaluated together. Although different morphological tumour types, such as solid, papillary, and alveolar, have been described, it may be difficult, and is of limited use, to subclassify the tumours based on histologic pattern, as two or more patterns can be present within the same tumour (Figs. 2.62 and 2.63).

Lung tumours have been induced in mice by a wide range of genotoxic and nongenotoxic compounds, including nitrosamines, metals, industrial chemicals, and pharmaceuticals. Many of these nongenotoxic

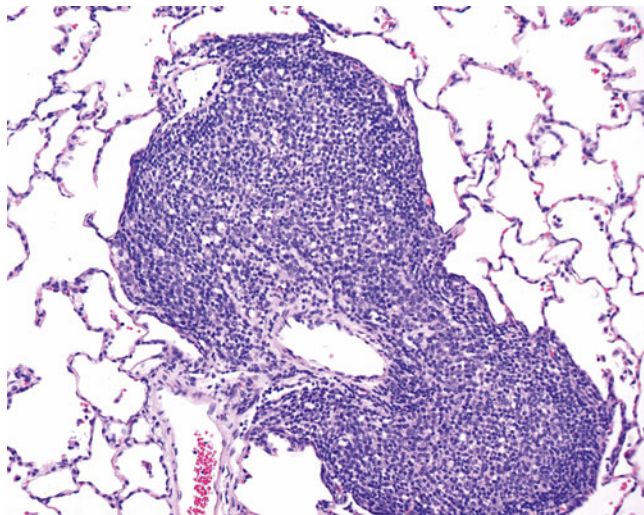


**FIGURE 2-57.** Marked perivascular lymphocytic infiltration is present in lung of this dog. The animal received an immunostimulant.



compounds, such as metronidazole, have been shown to be of no significance to humans at therapeutic doses. This is possibly because mice have larger numbers of Clara cells which contain a mouse-specific P450 isoform 2f2, resulting in higher levels of metabolism of many compounds and generation of metabolites that increase Clara cell turnover [38].

Squamous metaplasia in the lower conducting airways and alveoli occurs when proliferation of the existing cell type provides insufficient protection (Fig. 2.64). This occurs typically in response to inhalation of particulate matter, such as silica.

Along with squamous metaplasia, pulmonary keratinising cysts, cystic keratinising epitheliomas, and squamous cell carcinomas in rats form a continuum of lesions that are induced classically by prolonged exposure to inhaled particles or aerosols, such as talc, quartz, nickel oxide, and diesel exhaust. These changes result from initial squamous metaplasia of alveolar or bronchiolar cells, with subsequent neoplastic transformation and proliferation to form tumours. Morphologically, keratinising cysts are circumscribed cystic lesions lined by a layer of squamous epithelium without excessive

proliferative changes (Fig. 2.65). Cystic keratinising epitheliomas demonstrate peripheral growth into alveolar spaces, numerous mitoses, and proliferating walls. Squamous cell carcinomas are highly invasive, with varying degrees of differentiation and keratin formation (Fig. 2.66).

Mesotheliomas are caused by a range of agents in a number of species including man. Asbestos, fibrous silicates, and thorium dioxide are associated with these tumours in man. In addition to asbestos, many compounds including bromine-containing chemicals, nitrosourea, and acrylamide induce peritoneal mesotheliomas in F344 rats (Fig. 2.67).

In dog safety studies, focal pulmonary subpleural lesions which include alveolar fibrosis, macrophage aggregates, alveolar type II hyperplasia, and squamous metaplasia are a common background finding. The lesions are possibly related to old infections with *Filaroides* or *Toxocara* species [39] and are of no biological significance. However, a high incidence of these lesions in treated animals may be misinterpreted by pathologists unfamiliar with background pathology in laboratory beagles (Fig. 2.68).

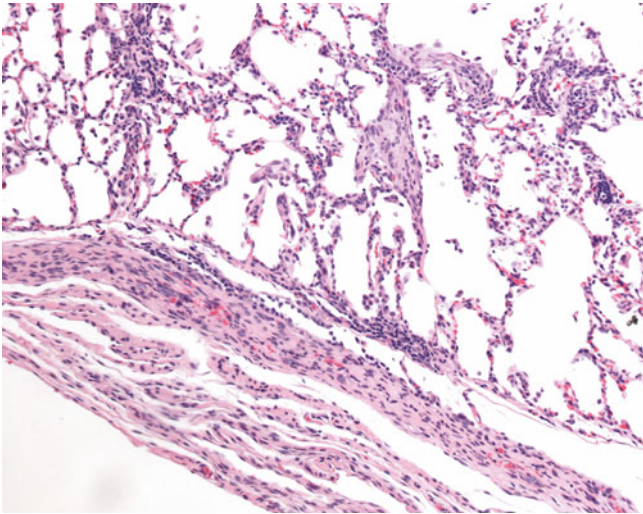


**FIGURE 2-58.** Pleural fibrosis of the lung in a rat treated with a PDE-4 inhibitor. Pleural collagen deposition, fibrosis, and adhesions are present. Mild alveolar inflammation and alveolar duct fibrosis are seen in the subpleural parenchyma. H&E.

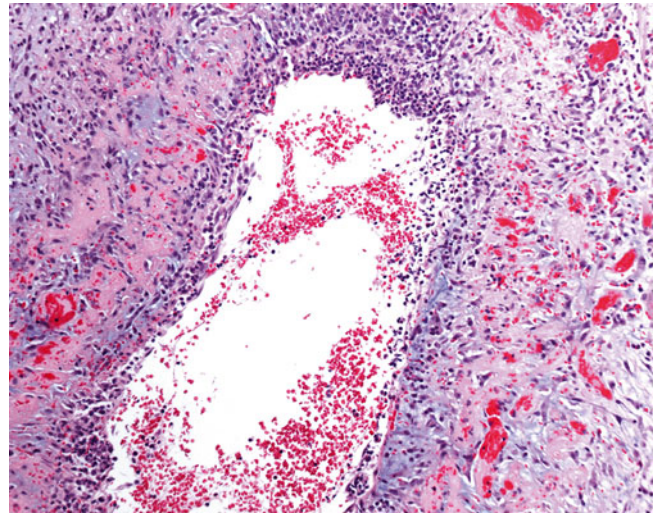


**FIGURE 2-59.** Necrotic vasculitis of a pulmonary vessel in a rat given a PDE-4 inhibitor. Severe fibrinoid mural necrosis and thickening of the vessel are seen, with marked inflammation and haemorrhage. These vasculitides are characteristic of PDE-4 inhibitors in rats. H&E.



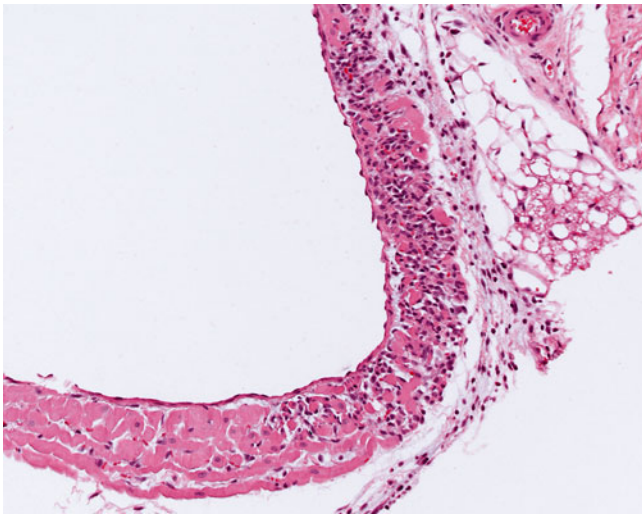


**FIGURE 2-60.** Pulmonary artery from a rat given an industrial chemical, showing focal degeneration of the myofibers. The affected fibres appear more eosinophilic and contracted, with loss of normal architecture. Associated lymphocytic and macrophage infiltration is present. H&E.

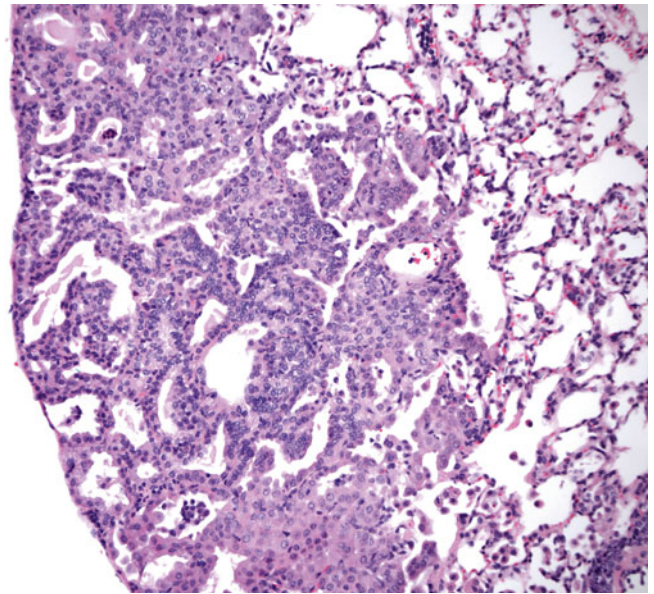


**FIGURE 2-61.** Bronchiolar alveolar hyperplasia in a mouse lung. Note the localised proliferation of large round cells thickening the alveolar septae. The lesion is too diffuse to qualify as an adenoma. H&E.

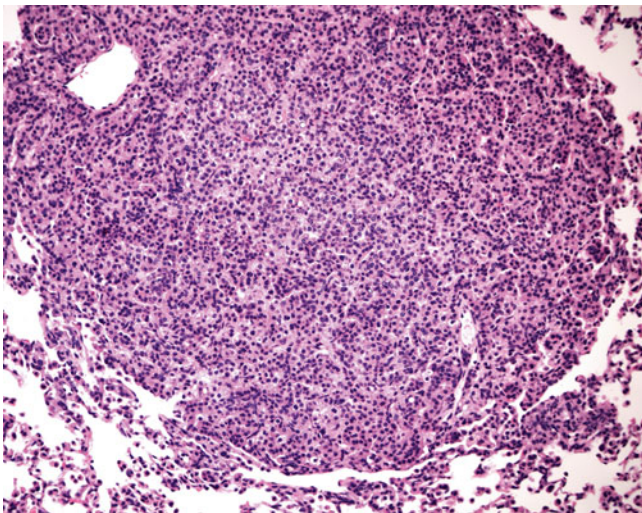


**FIGURE 2-62.** This bronchiolar-alveolar adenoma from a mouse lung is well circumscribed and solid. It is composed of well-differentiated round and cuboidal cells forming nests and acinar structures. H&E.

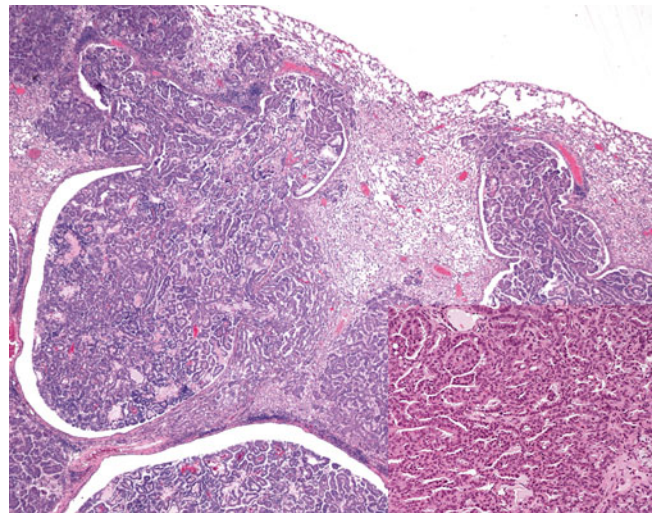


**FIGURE 2-63.** Bronchiolar-alveolar carcinoma in a mouse lung. This large, highly invasive tumour has invaded the airways. The tumour cells are basophilic and form papillary and acinar structures. H&E.



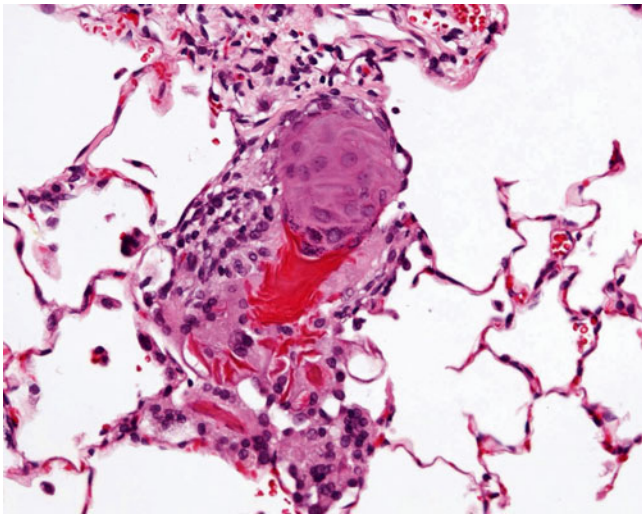


**FIGURE 2-64.** Focal squamous metaplasia of the alveolar wall, with keratin production. Coalescing aggregates of foamy macrophages are present around the lesion. H&E.

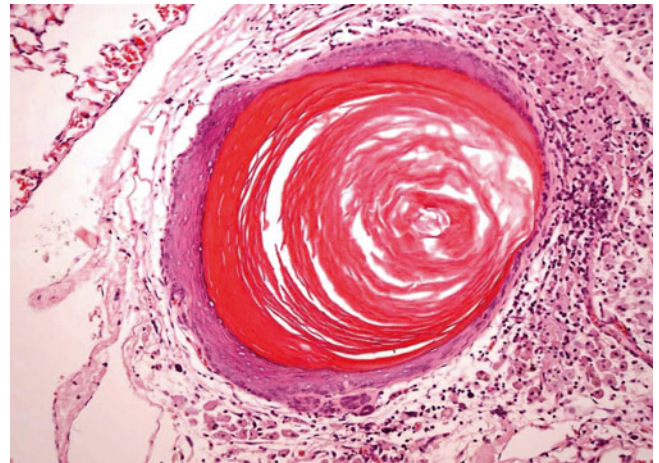


**FIGURE 2-65.** Keratin cyst in a rat lung, with foamy macrophage infiltration in the surrounding parenchyma. The cyst is lined by squamous epithelium of varying thickness and contains concentric lamellae of keratin. These are induced by particulate matter. H&E.

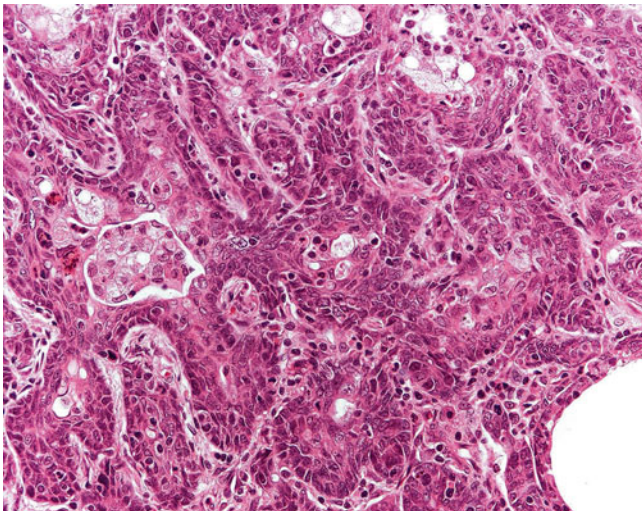


**FIGURE 2-66.** Squamous cell carcinoma from a rat lung. Large moderately differentiated epithelioid cells are forming nests, with spaces containing foamy macrophages. The tumour cells have large open nuclei, and several mitoses are evident. H&E.

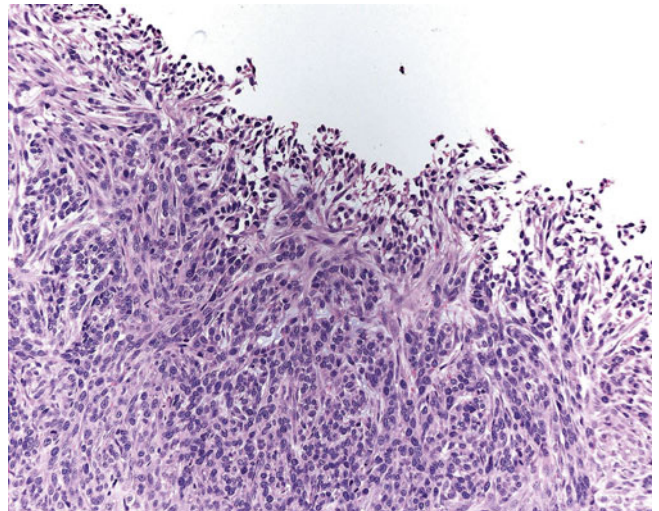


**FIGURE 2-67.** Malignant mesothelioma, from a mouse, which has invaded the thoracic wall. The tumour is composed of fronds and sheets of round and oval cells with large nuclei and scanty cytoplasm. Fibres are associated with development of these tumours. H&E.

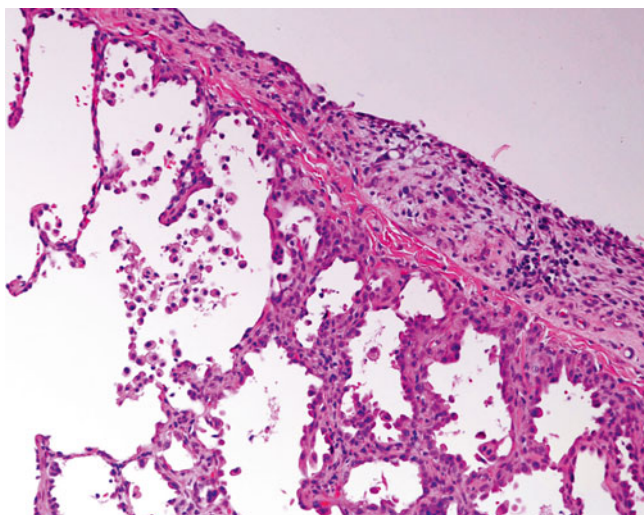


**FIGURE 2-68.** Fibrosing alveolitis in a dog. Pleural inflammation and thickening with subpleural alveolar fibrosis, as seen here, are typical of this lesion. Scattered foamy alveolar macrophages are present in the alveoli.

## References

1. Kimbell JS, Gross EA, Richardson RB, Conolly RB, Morgan KT. Correlation of regional formaldehyde flux predictions with the distribution of formaldehyde-induced squamous metaplasia in F344 rat nasal passages. *Mutat Res.* 1997;380:143–54.
2. Kimbell JS. Nasal dosimetry of inhaled gases and particles: where do inhaled agents go in the nose? *Toxicol Pathol.* 2006;34:270–3.
3. Kimbell JS, Gross EA, Joyner DR, Godo MN, Morgan KT. Application of computational fluid dynamics to regional dosimetry of inhaled chemicals in the upper respiratory tract of the rat. *Toxicol Appl Pharmacol.* 1993;121:253–63.
4. Kimbell JS, Godo MN, Gross EA, Joyner DR, Richardson RB, Morgan KT. Computer simulation of inspiratory airflow in all regions of the F344 rat nasal passages. *Toxicol Appl Pharmacol.* 1997;145:388–98.
5. Kimbell JS, Subramaniam RP, Gross EA, Schlosser PM, Morgan KT. Dosimetry modeling of inhaled formaldehyde: comparisons of local flux predictions in the rat, monkey, and human nasal passages. *Toxicol Sci.* 2001;64:100–10.
6. Kaewamatawong T, Kawamura N, Okajima M, Sawada M, Morita T, Shimada A. Acute pulmonary toxicity caused by exposure to colloidal silica: particle size dependent pathological changes in mice. *Toxicol Pathol.* 2005;33:743–9.
7. Harkema JR, Carey SA, Wagner JG. The nose revisited: a brief review of the comparative structure, function, and toxicologic pathology of the nasal epithelium. *Toxicol Pathol.* 2006;34:252–69.
8. Renne R, Brix A, Harkema J, Herbert R, Kittel B, Lewis D, et al. Proliferative and nonproliferative lesions of the rat and mouse respiratory tract. *Toxicol Pathol.* 2009;37:5S–73.
9. Young JT. Histopathologic examination of the rat nasal cavity. *Fundam Appl Toxicol.* 1981;1:309–12.
10. Morgan KT. Approaches to the identification and recording of nasal lesions in toxicology studies. *Toxicol Pathol.* 1991;19:337–51.
11. Kai K, Sahto H, Yoshida M, Suzuki T, Shikanai Y, Kajimura T, Furuhashi K. Species and sex differences in susceptibility to olfactory lesions among the mouse, rat and monkey following an intravenous injection of vincristine sulphate. *Toxicol Pathol.* 2006;34:223–31.
12. Harkema JR. Comparative aspects of nasal airway anatomy: relevance to inhalation toxicology. *Toxicol Pathol.* 1991;19:321–36.
13. Harkema JR. Comparative pathology of the nasal mucosa in laboratory animals exposed to inhaled irritants. *Environ Health Perspect.* 1990;85:231–8.
14. Buckley LA, Jiang XZ, James RA, Morgan KT, Barrow CS. Respiratory tract lesions induced by sensory irritants at the RD50 concentration. *Toxicol Appl Pharmacol.* 1984;74:417–29.
15. Monticello TM, Morgan KT, Uraih L. Nonneoplastic nasal lesions in rats and mice. *Environ Health Perspect.* 1990;85:249–74.
16. Lewis JL, Nikula KJ, Sachetti LA. Induced xenobiotic-metabolizing enzymes localized to eosinophilic globules in olfactory epithelium of toxicant-exposed F344 rats. *Inhal Toxicol.* 1994;6:422–5.
17. Renne RA, Gideon KM, Harbo SJ, Staska LM, Grumbein SL. Upper respiratory tract lesions in inhalation toxicology. *Toxicol Pathol.* 2007;35:163–9.
18. Genter MB, Owens DM, Deamer NJ. Distribution of microsomal epoxide hydrolase and glutathione S-transferase in the rat olfactory mucosa: relevance to distribution of lesions caused by systemically-administered olfactory toxicants. *Chem Senses.* 1995;20:385–92.
19. Genter MB, Deamer NJ, Blake BL, Wesley DS, Levi PE. Olfactory toxicity of methimazole: dose-response and structure-activity studies and characterization of flavin-containing monooxygenase activity in the Long-Evans rat olfactory mucosa. *Toxicol Pathol.* 1995;23:477–86.
20. Dejonghe S, Lammens L, Raoof A, Steemans K, Broeckaert F, Verbeeck J, et al. Lethal rhinitis/sinusitis in rodents by aspiration of formulation in gavage studies: importance of evaluation of the nose. *Exp Toxicol Pathol.* 2008;61:410.
21. Maronpot RR, Miller RA, Clarke WJ, Westerberg RB, Decker JR, Moss OR. Toxicity of formaldehyde vapor in B6C3F1 mice exposed for 13 weeks. *Toxicology.* 1986;41:253–6.
22. Takagi M, Shiraiwa K, Kusuoka O, Tamura K. A case of olfactory neuroblastoma induced in a rat by N-nitrosobis(2-hydroxypropyl)amine. *J Toxicol Pathol.* 2010;23:111–4.
23. Renne RA, Gideon KM. Types and patterns of response in the larynx following inhalation. *Toxicol Pathol.* 2006;34:281–5.
24. Lewis DJ. Morphological assessment of pathological changes within the rat larynx. *Toxicol Pathol.* 1991;19:352–7.
25. Lewis DJ, Prentice DE. The ultrastructure of rat laryngeal epithelia. *J Anat.* 1980;130:617–32.



26. Kaufmann W, Bader R, Ernst H, Harada T, Hardisty J, Kittel B, et al. 1st international ESTP expert workshop: "Larynx squamous metaplasia." A re-consideration of morphology and diagnostic approaches in rodent studies and its relevance for human risk assessment. *Exp Toxicol Pathol*. 2009;61:591–603.
27. Osimitz TG, Droege W, Finch JM. Toxicologic significance of histologic change in the larynx of the rat following inhalation exposure: a critical review. *Toxicol Appl Pharmacol*. 2007;225:229–37.
28. Kambara T, McKeivitt TP, Francis I, Woodfine JA, McCawley SJ, Jones SA, et al. Eosinophilic inclusions in rat Clara cells and the effect of an inhaled corticosteroid. *Toxicol Pathol*. 2009;37:315–23.
29. Sturgess J, Reid L. The effect of isoprenaline and pilocarpine on (a) bronchial mucus-secreting tissue and (b) pancreas, salivary glands, heart, thymus, liver and spleen. *Br J Exp Pathol*. 1973;54:388–403.
30. Haworth R, Woodfine J, McCawley S, Pilling AM, Lewis DJ, Williams TC. Pulmonary neuroendocrine cell hyperplasia: identification, diagnostic criteria and incidence in untreated ageing rats of different strains. *Toxicol Pathol*. 2007;35:735–40.
31. Sunday ME, Willett CG. Induction and spontaneous regression of pulmonary neuroendocrine cell hyperplasia in a hamster model. *Chest*. 1992;101:21S.
32. Gopinath C, Prentice DE, Lewis DJ. Atlas of experimental toxicological pathology. Lancaster: MTP Press Limited; 1987. p. 11–22.
33. Oslund KL, Hyde DM, Putney LF, Alfaro MF, Walby WF, Tyler NK, et al. Activation of calcitonin gene-related peptide receptor during ozone inhalation contributes to airway epithelial injury and repair. *Toxicol Pathol*. 2009;37:805–13.
34. Oslund KL, Hyde DM, Putney LF, Alfaro MF, Walby WF, Tyler NK, et al. Activation of neurokinin-1 receptors during ozone inhalation contributes to epithelial injury and repair. *Am J Respir Cell Mol Biol*. 2008;39:279–88.
35. Smith BR, Brian WR. The role of metabolism in chemical-induced pulmonary toxicity. *Toxicol Pathol*. 1991;19:470–81.
36. Zhang J, Wenthold Jr RJ, Yu ZX, Herman EH, Ferrans VJ. Characterization of the pulmonary lesions induced in rats by human recombinant interleukin-2. *Toxicol Pathol*. 1995;23:653–66.
37. Pilling AM, Mifsud NA, Jones SA, Endersby-Wood HJ, Turton JA. Expression of surfactant protein mRNA in normal and neoplastic lung of B6C3F1 mice as demonstrated by in situ hybridization. *Vet Pathol*. 1999;36:57–63.
38. Strupp C, Banas DA, Cohen SM, Gordon EB, Jaeger M, Weber K. Relationship of metabolism and cell proliferation to the mode of action of fluensulfone-induced mouse lung tumors: analysis of their human relevance using the IPCS framework 1. *Toxicol Sci*. 2012;128:284–294.
39. Scudamore C. Beagle dog. In: McInnes EF, editor. Background lesions in laboratory animals: a colour atlas. Edinburgh: Saunders Elsevier; 2012. p. 37–44.

Atlas of Toxicological Pathology

Gopinath, C.; Mowat, V.

2014, XI, 285 p. 300 illus., 200 illus. in color., Hardcover

ISBN: 978-1-62703-997-0

A product of Humana Press